Miner Deposita (2006) 41: 691–711
DOI 10.1007/s00126-006-0086-2

ARTICLE

Melissa J. Gregory

Copper mobility in the Eastern Creek Volcanics, Mount Isa, Australia: evidence from laser ablation ICP-MS of iron-titanium oxides

Received: 5 May 2005 / Accepted: 4 August 2006 / Published online: 27 September 2006

Abstract The Palaeoproterozoic Eastern Creek Volcanics are a series of copper-rich tholeiitic basalts which occur adjacent to the giant sediment-hosted Mount Isa copper deposit in Queensland, Australia. The volcanic rocks are often cited as the source of metals for the deposit. New laser ablation ICP-MS analyses of iron–titanium oxides from the basalts provide evidence for the local mobilisation of copper during regional greenschist facies metamorphism. This interpretation is based on the observation that copper-bearing magmatic titanomagnetite was destabilised during greenschist facies metamorphism, and the new magnetite which crystallised was copper poor. Petrological observations, regional geochemical signatures and geochemical modelling suggest that the mobilised copper was concentrated in syn-metamorphic epidote-rich alteration zones, creating a pre-concentration of copper before the main mineralisation event at Mount Isa. Geochemical modelling demonstrates this process is enhanced by the addition of CO_2 from adjacent carbonate-rich sediments during metamorphic devolatilisation. Regional geochemical data illustrate elevated copper concentrations in epidote-rich zones (high CaO), but where these zones are overprinted by potassic alteration (high K_2O), copper is depleted. A two-stage model is proposed whereby after metamorphic copper enrichment in epidote–titanite alteration zones, an oxidised potassium-rich fluid leached copper from the epidote-altered metabasalts and deposited it in the overlying sedimentary rocks to form the Mount Isa copper deposit. This ore-forming fluid is expressed regionally as potassium feldspar-rich veins and locally as biotite-rich alteration, which formed around major fluid conduits between the metabasalt metal source rocks and the overlying deposit host sequence. This model is consistent with the remobilisation of copper from mafic source rocks, as has been found at other world-class copper deposits.

Keywords Eastern Creek Volcanics · Mount Isa · Australia · Copper · Iron–titanium oxide geochemistry · Laser ablation ICP-MS

Editorial handling: B. Gemmell

Electronic supplementary material Supplementary material is available in the online version of this article at http://dx.doi.org/10.1007/s00126-006-0086-2 and is accessible for authorized users.

M. J. Gregory (✉)
pmd*CRC, School of Geosciences, Monash University,
P.O. Box 28E Clayton, Melbourne, Victoria, Australia
e-mail: Melissa.Gregory@sci.monash.edu.au
Fax: +61-3-99054903

Introduction

The Mount Isa copper deposit, in Queensland, Australia, is one of the world's largest accumulations of sediment-hosted copper. The orebody contains over 13 million tonnes of Cu at 3.3 wt% (Perkins 1990), hosted by a chalcopyrite–pyrrhotite ore assemblage, within a discordant syntectonic breccia system (Swager 1985). The majority of authors interpret the Mount Isa copper deposit to be both post-peak metamorphic in age and hydrothermal in origin (e.g. Perkins 1984; Swager 1985; Waring 1990; Valenta 1994). However, the source of copper has been the subject of many studies, and this paper aims to provide additional constraints on this topic.

The Mount Isa copper deposit is a unique style of deposit which cannot be categorised as a typical sediment-hosted copper deposit. This is due predominantly to the relatively high temperatures of ore formation at Mount Isa compared with the low temperatures associated with many sediment-hosted deposits (Waring et al. 1998).

The Mount Isa deposit occurs adjacent to an 8-km-thick sequence of copper-rich tholeiitic basalts (the Eastern Creek Volcanics) which have been proposed as the source of copper (Smith and Walker 1971; Wilson et al. 1985; Hannan et al. 1993; Heinrich et al. 1995). The basalts of the Eastern Creek Volcanics are copper-depleted close to the Mount Isa deposit. Several authors have suggested models, based on alteration studies, whereby oxidised fluids circulated through the volcanic rocks via major structures, leaching copper which was then deposited in the overlying

sedimentary rocks (Wyborn 1987; Bain et al. 1992; Hannan et al. 1993; Heinrich et al. 1995).

This paper aims to expand on previous alteration studies at Mount Isa by presenting new petrological and mineral chemical data for metabasalts, which demonstrate copper mobility within the metabasalts. Along with regional geochemistry and geochemical modelling, this work demonstrates how copper can be mobilised from basalts and concentrated into permeable zones during metamorphism, and later remobilised by circulating oxidised fluids associated with ore deposition at Mount Isa. This two-stage model allows fluids to leach copper from the majority of the volcanic pile, away from the major fluid conduits proposed by previous studies, and hence, copper can be mobilised from a much larger source region.

Geological setting

The Leichhardt River Fault Trough of the Western Fold Belt in the Mount Isa Inlier is dominated by mafic igneous rocks of the Haslingden Group (Fig. 1), which were deposited in an intracontinental rift setting during the Palaeoproterozoic (Wilson et al. 1985). The Haslingden Group consists of the coarse sandstone (and lesser quartzite) of the Mount Guide Quartzite and intercalated metabasalts and metasedimentary rocks of the Eastern Creek Volcanics (e.g. Blake and Stewart 1992). Two attempts to date the metabasalts of the Eastern Creek Volcanics have yielded differing estimates: 1,710±25 Ma using whole rock Pb–Pb (Gulson et al. 1983) and 1,807±78 Ma using whole rock Th–Pb (Farquharson and Richards 1974). The maximum depositional age of the Lena Quartzite, which separates the two members of the Eastern Creek Volcanics, is 1,779±4 Ma (SHRIMP zircon age, Neumann et al. 2005).

The Haslingden Group rocks were intruded by the Sybella Batholith (Fig. 1), resulting in contact metamorphism which affected significant areas of the Eastern Creek Volcanics west of the Mount Isa Fault (Rubenach 1992). Currently, the best estimate of emplacement age for the Sybella Batholith is provided by SHRIMP zircon ages of 1,675 to 1,655 Ma (Connors and Page 1995; Page et al. 2000; Neumann et al. 2005).

The Mount Isa Group, which overlies the Haslingden Group at Mount Isa, is a thick (4.5 to 6.0 km) sequence of carbonaceous and dolomitic siltstones, mudstones and shales, which were deposited under shallow water conditions (Muir 1981; Neudert and Russell 1981; Painter et al. 1999). The Urquhart Shale of the upper Mount Isa Group consists of interbedded siltstones and shales and hosts the Mount Isa copper deposit and the lead–zinc deposits at

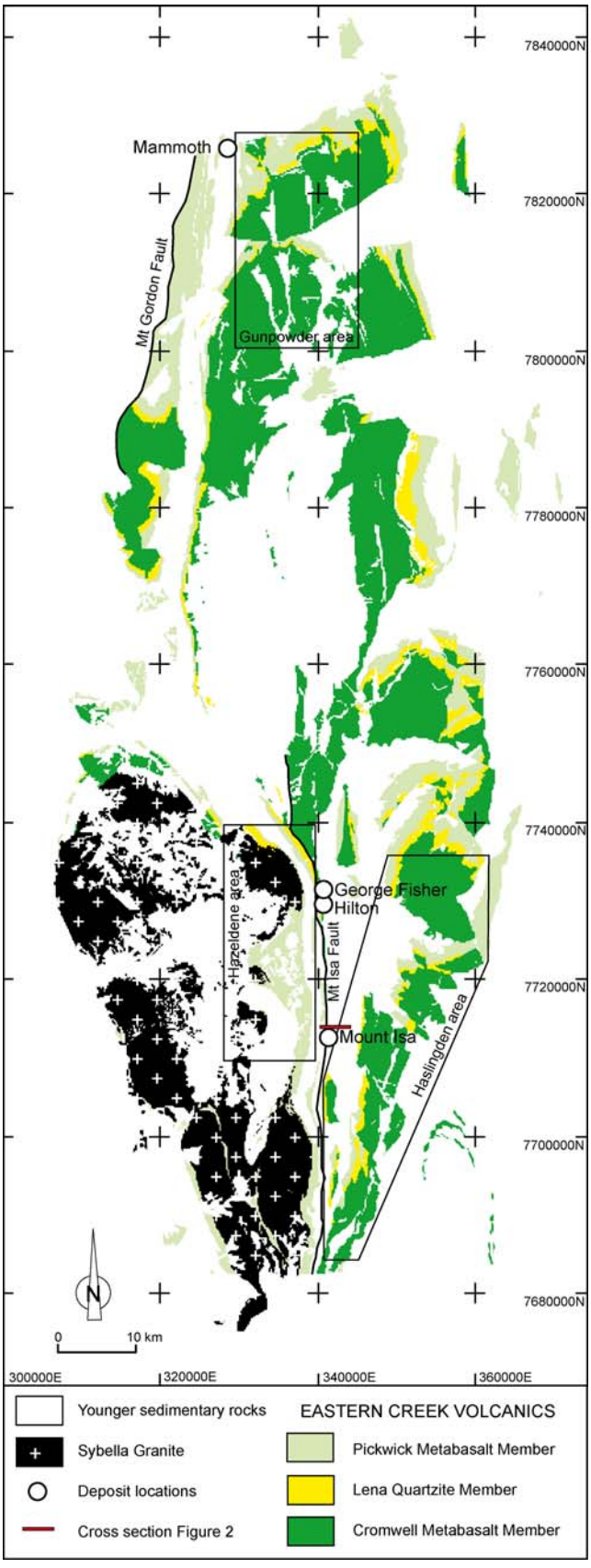

Fig. 1 Regional surface extent of the Eastern Creek Volcanics around Mount Isa, indicating the different study areas—Gunpowder, Haslingden and Hazeldene, and the location of major mineral deposits including Mount Isa Cu and Pb–Zn, Hilton Pb–Zn, George Fisher Pb–Zn and Mammoth Cu deposits. Geology adapted from the Mary Kathleen and Mount Isa 1:100,000 sheets (Derrick 1976 and Hill 1978, respectively)

Mount Isa, Hilton and George Fisher. Tuff marker beds within the Urquhart Shale indicate that these rocks were deposited at 1,652±7 and 1,655±4 Ma based on SHRIMP zircon ages (Page and Sweet 1998; Page et al. 2000).

The Mount Isa region underwent deformation during the Isan Orogeny between 1,590 and 1,500 Ma (O'Dea et al. 1997). D_2 represents the most widespread phase of the Isan Orogeny, with east–west compression accompanied by low-P, high-T metamorphism (Connors et al. 1992; Rubenach 1992). This deformation resulted in north–south striking upright F_2 folds and a pervasive north–south trending S_2 cleavage (Connors et al. 1992; Rubenach 1992; O'Dea et al. 1997). The absolute age of peak metamorphism in the Western Fold Belt is constrained at around 1,575 Ma (Hand and Rubatto 2002; Duncan et al. 2006).

A later period of tectonism (D_4 of Connors et al. (1992) or D_3 of Lister et al. (1999) and most other studies) is characterised by northeast–southwest shortening and west over east fault movement resulting in north–northwest oriented folds, major ductile shear zone development, as well as reactivation and dilation of pre-existing structures (Connors et al. 1992; Rubenach 1992; O'Dea et al. 1997; Lister et al. 1999). This event is synchronous with copper deposition at Mount Isa (Perkins 1984; Swager 1985; Valenta 1994).

Eastern Creek Volcanics

The Eastern Creek Volcanics outcrop over an area of 150×40 km (Fig. 1), with a maximum measured thickness of over 7 km (Blake and Stewart 1992). The Eastern Creek Volcanics are a series of subalkaline continental tholeiitic basalts (Wilson et al. 1985). The sequence is divided into three members, the lower Cromwell Metabasalt Member, the Lena Quartzite and the upper Pickwick Metabasalt Member. Individual basalt flows have a massive medium- to coarse-grained basal portion that fines upwards into an amygdaloidal zone and that is locally capped by flow top breccias (Wilson et al. 1985; Bain et al. 1992).

Metabasalts from the Gunpowder area, 120 km north of Mount Isa, are the most pristine basalts found in the region as illustrated by the geochemical study of Wilson et al. (1985) and by the preservation of magmatic textures and relict magmatic minerals. Regional metamorphism in the Gunpowder area only reached lower greenschist facies. The average copper concentration for the Cromwell Metabasalt in the Gunpowder area has been reported as 229 ppm (Wilson et al. 1985) compared with an average of 152 ppm for tholeiitic continental flood basalts worldwide (Crocket 2002). The Pickwick Metabasalt Member is derived from a less evolved magma that is MgO rich and relatively copper poor (average of 142 ppm Cu: Wilson et al. 1985) compared with the Cromwell Metabasalt Member.

A study by Gregory et al. (in preparation) interpreted platinum-group element and trace element geochemical data which suggested that the Eastern Creek Volcanics evolved from a copper-rich mantle source. Limited sulphide formation in the parent magmas resulted in copper behaving as an incompatible element during igneous differentiation, becoming enriched in the basalts with progressive fractionation (Gregory et al., in preparation). The Cromwell Member represents the most fractionated and, therefore, the copper-rich part of the sequence. The strong correlation between MgO and copper in the Gunpowder area reflects magmatic fractionation and is consistent with basalts in this area preserving their primary magmatic copper content (Gregory et al., in preparation). The sulphide-poor nature of the magma suggests that the majority of copper is not hosted in magmatic sulphides and has been incorporated into other oxide and silicate phases.

Regional D_2 metamorphism of the Eastern Creek Volcanics around Mount Isa has resulted in several different mineral assemblages. To the west of Mount Isa, in the Hazeldene area (Fig. 1), the Eastern Creek Volcanics have undergone amphibolite facies metamorphism resulting in hornblende-dominated amphibolites. Trace element geochemistry indicates that the Pickwick Metabasalt Member dominates the amphibolite sequence west of the Mount Isa Fault (Bultitude and Wyborn 1982). East of Mount Isa in the Haslingden area (Fig. 1), the Cromwell Metabasalt Member dominates the sequence and has undergone greenschist facies metamorphism.

The Haslingden area metabasalts have been the subject of extensive alteration studies by Wyborn (1987), Bain et al. (1992), Hannan et al. (1993) and Heinrich et al. (1995). These studies provide an alteration framework for the Eastern Creek Volcanics east of the Mount Isa Fault (Table 1). These authors found that the oldest alteration assemblage is albite–actinolite, which resulted from D_1 to early-D_2 regional metamorphism or possibly syn-eruption hydrothermal alteration (Wyborn 1987; Bain et al. 1992). Albite–actinolite assemblages were overprinted by two peak metamorphic (D_2) mineral assemblages: calcite–magnetite and epidote–titanite. All three assemblages were subsequently overprinted by chlorite in the mine environment and intense carbonate–Fe oxide alteration away from the mine. The western portion of the Haslingden area is dominated by albite–actinolite and calcite–magnetite alteration, and the eastern area is dominated by epidote–titanite alteration (Wyborn 1987).

The Eastern Creek Volcanics are in fault contact with the Mount Isa copper deposit and its host sedimentary rocks, the Urquhart Shale (Fig. 2). The trends displayed by incompatible elements, such as Y, Zr and Nb, and rare earth element geochemical data, have been used to demonstrate that the metabasalts below the copper deposit belong to the Cromwell Metabasalt Member (Hannan et al. 1993).

This study will concentrate on the petrology and iron-oxide geochemistry of metabasalt drill-core samples below the Mount Isa copper deposit (mine section 38,000 mN; Fig. 2) and amphibolite samples from the Hazeldene area to the west of Mount Isa. The results will be used to interpret regional geochemistry datasets from the Haslingden and Hazeldene areas (Fig. 1).

Table 1 Alteration assemblages described by previous studies[a]

Albite–actinolite alteration	Epidote–titanite alteration	Calcite–magnetite alteration	Chlorite–albite alteration	Relationship to copper	Publication
Low-grade metamorphosed basalts with relict clinopyroxene, labradorite and some opaque phases.	Not described	Not described	Zone of Mg-rich chlorite found parallel to the Paroo Fault. Rocks show extreme copper depletion.	Copper depletion associated with K_2O, MgO and CO_2 enrichment	Wilson et al. 1985: Geochemical study of the Eastern Creek Volcanics in the Gunpowder area
Metabasalts are uncleaved and have relict igneous textures with traces of igneous plagioclase, clinopyroxene, ilmenite and magnetite which are being progressively replaced by albite, actinolite and chlorite. This alteration type forms 70% of the Gunpowder area and 30% of the area east of Mount Isa. *Timing—pre-D_2, either D_1 or at eruption*	Metabasalts which are folded, faulted and/or cleaved are dominated by epidote and titanite with albite, actinolite and chlorite. This alteration dominates the Eastern Creek Volcanics in the eastern half of the Haslingden area, forming only near faults and fractures in the Gunpowder area. *Timing—D_2*	Metabasalts are deformed and dominated by calcite, albite, chlorite and magnetite. Assemblage formed by the replacement of epidote assemblages due to the interaction with CO_2-rich fluids. Alteration is rare in the Gunpowder area but dominates the western half of the Haslingden area. Common near major faults and carbonate-rich members of the Mount Isa Group. *Timing—late D_2 as overprints epidote–titanite alteration*	Strongly cleaved rocks dominated by chlorite–albite–rutile. Restricted to zone under the Mount Isa mine. *Timing—D_3*	Copper depletion associated with cleavage formation and faulting in the metabasalts	Wyborn 1987: Summary of the petrology and geochemistry of alteration types in the Eastern Creek Volcanics east of the Mount Isa Fault
Metabasalts contain albite after plagioclase, chlorite–epidote clots after pyroxene and titanite-rimmed magnetite after titanomagnetite.	Two types of epidote alteration. Epidote in flow-top breccias is interpreted to be either product of metamorphic metasomatism or syn-eruptive/burial-related hydrothermal alteration. Veining-related epidote alteration occurs as closely spaced stacked epidote veins or epidote as diffuse halos up to 1 m wide around quartz(–epidote–calcite) veins. *Timing—some veins cut the metamorphic cleavage and others are boundinaged by it, therefore interpreted as syn-D_2.*	Described as carbonate–iron-oxide alteration which is found in intense km scale north–south orientated shatter zones. Intense variety of calcite–magnetite alteration of Wyborn (1987). Shatter zones cut the D_2 cleavage, and the most intensely altered rocks are dominated by calcite–albite–magnetite–hematite–quartz. Veining characterised by calcite (–quartz–chlorite). *Timing—post-D_2*	Not described	Timing of carbonate–Fe-oxide alteration and fluid inclusion compositions coincide with copper deposition. Carbonate–Fe-oxide alteration zones represent channels for downward-flowing fluids, which interact with the Eastern Creek Volcanics, scavenging copper before ascending into the overlying sedimentary rocks to form the Mount Isa copper deposit.	Bain et al. 1992: Stratigraphic, structural and alteration study including the Eastern Creek Volcanics in the Haslingden area

Not described	Epidote alteration is associated with zones of high permeability such as fractures and flow tops. Alteration zones occur as 5 to 50 m thick flow top breccia horizons or as swarms up to 50 m wide of vertical 10–40 cm planar sheets within the deformed hinge zones of D_2 folds. Epidote–quartz veins common in both types. Copper is depleted in some samples and anomalously high in others. *Timing—D_2*	Not described	Described as chlorite schist found below the Paroo Fault. Rocks dominated by chlorite–rutile and lesser ilmenite. Albite relicts are truncated by anastomosing chlorite, while titanite is replaced by ilmenite and rutile. Bands of ilmenite-bearing biotite schist are found within chlorite schist increasing in volume towards regional metabasalts. *Timing—post-D_2*	Hydrothermal fluids flowing along/up the Paroo Fault formed chlorite schist and scavenged copper to form the Mount Isa copper deposit.	Hannan et al. 1993: Alteration study of the Eastern Creek Volcanics below and east of the Mount Isa copper deposit
Not described	Descriptions taken from Wyborn (1987), Bain et al. (1992) and Hannan et al. (1993). Epidote alteration affects 10% of the outcrop area east of Mount Isa. Epidote-altered samples have generally lost copper, but some show copper enrichment. *Timing—overlaps in time with regional metamorphism and deformation (D_2)*	Carbonate–iron-oxide alteration descriptions taken from Wyborn (1987) and Bain et al. (1992). Some intense zones are up to 500 m wide and continuous over 5 km. Copper is lost from some samples but gained by others. *Timing—post-D_2*	Rocks described as Mg chlorite–rutile and characterised by Mg chlorite–quartz–albite–rutile. Mg-rich biotite, pyrrhotite and ilmenite occur locally. Geochemistry shows copper depletion. *Timing—overlaps or post-dates carbonate–Fe-oxide alteration, post-D_2*	As for Bain et al. (1992). Oxidised fluids from above flowed down through carbonate–iron-oxide zones, leaching copper from the Eastern Creek Volcanics and depositing it in the reduced sedimentary rocks of the Urquhart Shale.	Heinrich et al. 1995: Alteration study building on Wyborn 1987 and Bain et al. 1992, concentrating on the Haslingden area

[a]Nomenclature after Wyborn (1987)

Sample petrology

Mine area

Mine section 38,000 mN (Fig. 2) occurs at the northern end of the Mount Isa copper deposit. Chalcopyrite–pyrrhotite mineralisation occurs in this area but is not included within the currently mineable resource. Drilling on this northing includes deep diamond holes that cover significant vertical extent of the Eastern Creek Volcanics below the Paroo Fault and allows for the correlation of lithology and alteration assemblages within the volcanic sequence. The Eastern Creek Volcanics have undergone greenschist facies metamorphism in the mine area, and alteration assemblages are described using the framework of previous studies (Table 1), with particular reference to the Fe–Ti oxides.

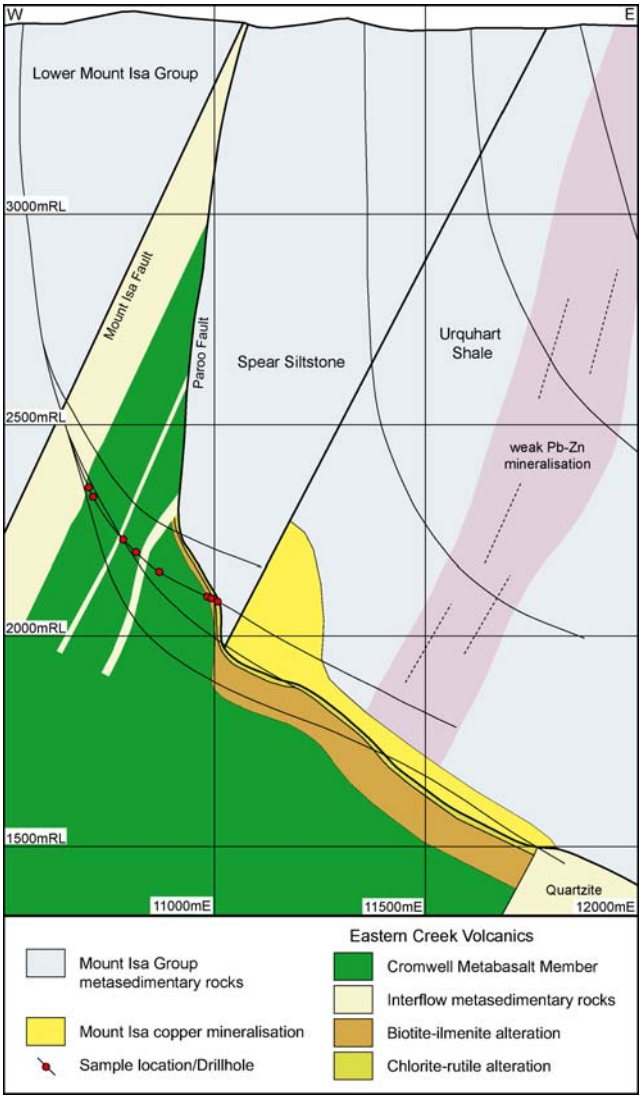

Fig. 2 Mount Isa mine section 38,000 mN showing the juxtaposition of the Eastern Creek Volcanics and Mount Isa Group sedimentary rocks, which host the Mount Isa Cu and Pb–Zn deposits. Location of section shown in Fig. 1. Interpretation based on geological model of Xstrata Copper with detail provided by drill-core logging by the author

Albite–actinolite assemblages

The oldest documented mineral assemblages, the albite–actinolite-dominated metabasalts, are found in areas distal to faults, fractures and interflow sedimentary rocks (Fig. 3) and are characterised by medium- to fine-grained masses of actinolite and titanomagnetite with a finer-grained (chlorite, albite ± epidote) groundmass. Actinolite and chlorite have pseudomorphed igneous pyroxenes, consistent with the greenschist facies metamorphism of mafic volcanic rocks. The metabasalts are, in different areas, fine grained, due to rapid cooling of the lavas, and coarse grained, suggesting slower cooling towards the centre of individual basalt flows.

The main opaque phase in the coarser grained samples is titanomagnetite, with central lamellae of ilmenite producing a 'sandwich-type' texture (Fig. 4a). Ilmenite lamellae are not present in the equivalent finer grained metabasalts, possibly due to fast cooling of the basalt (Fig. 4b). Very fine (<1 μm) exsolution lamellae occur within all titanomagnetites, the former typically formed during cooling (Frost and Lindsley 1991). Titanite occurs as rims around titanomagnetite grains. Also, titanite alteration of the titanium-rich exsolution lamellae of the titanomagnetite is common. Alteration progressed further in finer grained metabasalt (cf. Fig. 4a with b).

Magnetite occurs as rare fine-grained, euhedral crystals in the groundmass and also as overgrowths on titanomagnetite (Fig. 4a,b). Minor chalcopyrite is the principal sulphide and is commonly intergrown with fine-grained epidote and K-feldspar which are minor phases within the metabasalt groundmass. One sample shows chalcopyrite inclusions in titanite rims around ilmenite (Fig. 4c).

Calcite–magnetite assemblages Metabasalts that have undergone calcite–magnetite alteration are found adjacent to interflow sedimentary rocks in the Eastern Creek Volcanics (Fig. 3). These metabasalts are fine grained, consisting of chlorite, albite and calcite with minor epidote (as fine crystals within large chlorite crystals). Calcite and quartz are found aligned within the peak metamorphic foliation and in pressure shadows around coarse-grained oxide phases.

Titanomagnetite is the dominant oxide phase with very fine titanium-rich exsolution lamellae which are typically altered to titanite (Fig. 4d). Fine- to medium-grained, euhedral magnetite crystals (Fig. 4d) occur extensively throughout these metabasalts.

A systematic change occurs from albite–actinolite alteration that preserved titanomagnetite through calcite–magnetite assemblages where new magnetite formed at the expense of titanomagnetite. Wyborn (1987) suggested that calcite–magnetite assemblages formed due to interaction of CO_2-rich fluids, which were sourced from the adjacent carbonaceous sedimentary rocks during regional metamorphism. The spatial relationship between calcite–magnetite assemblages and interflow sedimentary rocks found in this study supports this interpretation.

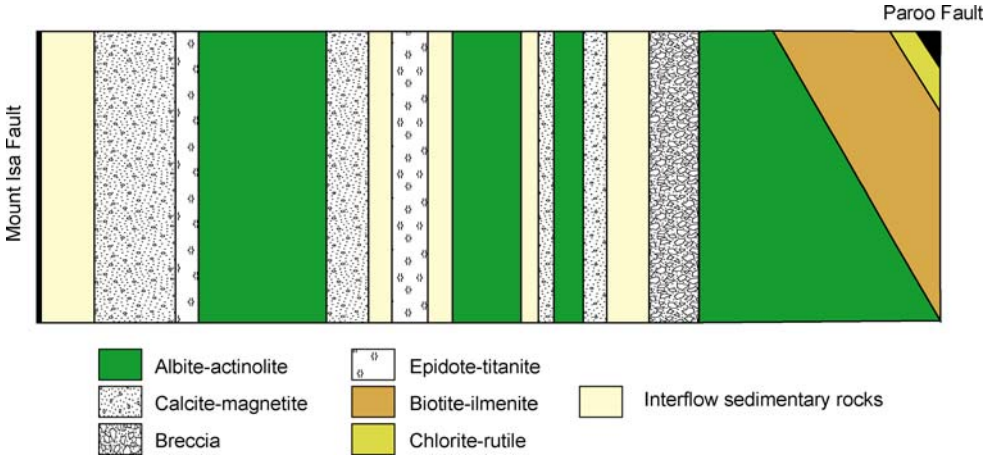

Fig. 3 Schematic east–west section through metabasalts on section 38,000 mN (Fig. 2) showing spatial relationships between interflow sedimentary rocks, alteration assemblages and the Paroo Fault

Chalcopyrite is found in association with magnetite, quartz and epidote, although its paragenetic relationship to these minerals is ambiguous. Calcite–chalcopyrite veins occur parallel to the metamorphic foliation (S_2) and have been boudinaged, with the chalcopyrite occurring in the vein selvedge within the metabasalt. This is consistent with an early-D_2 timing.

At Mount Isa, an unusual breccia occurs at the top of some metabasalt flows, especially adjacent to interflow sedimentary rocks (Fig. 3). The breccia contains rounded clasts dominated by magnetite, albite and titanite in a matrix of calcite, titanite and chlorite (Fig. 5a). Clasts are dominated by clusters of fine-grained, euhedral magnetite crystals (Fig. 4e). This assemblage is interpreted to be the product of an intense variety of calcite–magnetite alteration, which affected high permeability zones at the top of metabasalt flows. These zones may represent original igneous flow-top breccias within the basalt sequence, but the original angular breccia characteristics have been destroyed by the intense metasomatism.

Epidote–titanite assemblages

Metabasalts dominated by epidote–titanite assemblages are associated with high-permeability zones, such as fractures and contacts with interflow sedimentary rocks (Fig. 3). The alteration along these zones has resulted in abundant epidote growth with lesser quartz and titanite. Epidote is Fe rich, an observation also made by Heinrich et al. (1995). Titanite is part of the metabasalt groundmass and is the result of the breakdown of pre-existing titanomagnetite. A correlation between epidote alteration and zones of high permeability is well documented in the Eastern Creek Volcanics and many other mafic volcanic sequences (Hannan et al. 1993 and references therein).

Fine chalcopyrite grains within the metabasalt are associated with epidote and/or K-feldspar. Regionally, some vesicles are lined with epidote crystals which enclose grains of chalcopyrite, paragenetically followed by chlorite and finally calcite (Fig. 5b). The texture is interpreted to indicate that chalcopyrite precipitation occurred during epidote alteration of the volcanic sequence.

Biotite–ilmenite and chlorite–rutile assemblages

Based on diamond drill-core logging and petrographical studies, chlorite schist alteration below the Paroo Fault in the Mount Isa mine area can be divided into two assemblages (Figs. 2 and 3), a feature also described by Hannan et al. (1993). The outer region is dominated by biotite and ilmenite (10–65 m wide), and an inner region against the fault is dominated by chlorite and rutile (~10 m wide). The entire alteration zone is only prominent (more than 70 m wide) adjacent to copper mineralisation (Fig. 2), and this suggests a genetic relationship between this alteration and mineralisation.

Biotite–ilmenite samples have a groundmass of chlorite, albite and ilmenite, which has been overprinted by a fine network of biotite veinlets (Fig. 5c). The ilmenite has overgrown pre-existing titanomagnetite grains, in a manner such that the exsolution texture is preserved by titanite (Fig. 4f). Both ilmenite and biotite have overprinted albite and titanite, a relationship that indicates a post-metamorphic timing, and the close association of ilmenite and biotite suggests synchronous growth; this was also documented by Hannan et al. (1993).

Grains of calcite are totally enclosed by ilmenite in some cases, which is consistent with the overprinting of calcite–magnetite assemblages. Fine chalcopyrite crystals are associated with chlorite, and sub-micron inclusions of chalcopyrite within ilmenite crystals have been identified. Samples from the chlorite–rutile zone are dominated by chlorite, albite, ilmenite and rutile. Rutile has pseudomorphed ilmenite crystals.

K-feldspar veining

A population of veins found in metabasaltic rocks of the mine area contain K-feldspar, calcite, quartz and, locally, chalcopyrite (Fig. 5d,e). These veins are thin (typically less than 5 mm) and, although commonly found throughout the metabasalt sequence, are not prominent in appearance due to their fine nature. Such veins have not been previously described from Mount Isa.

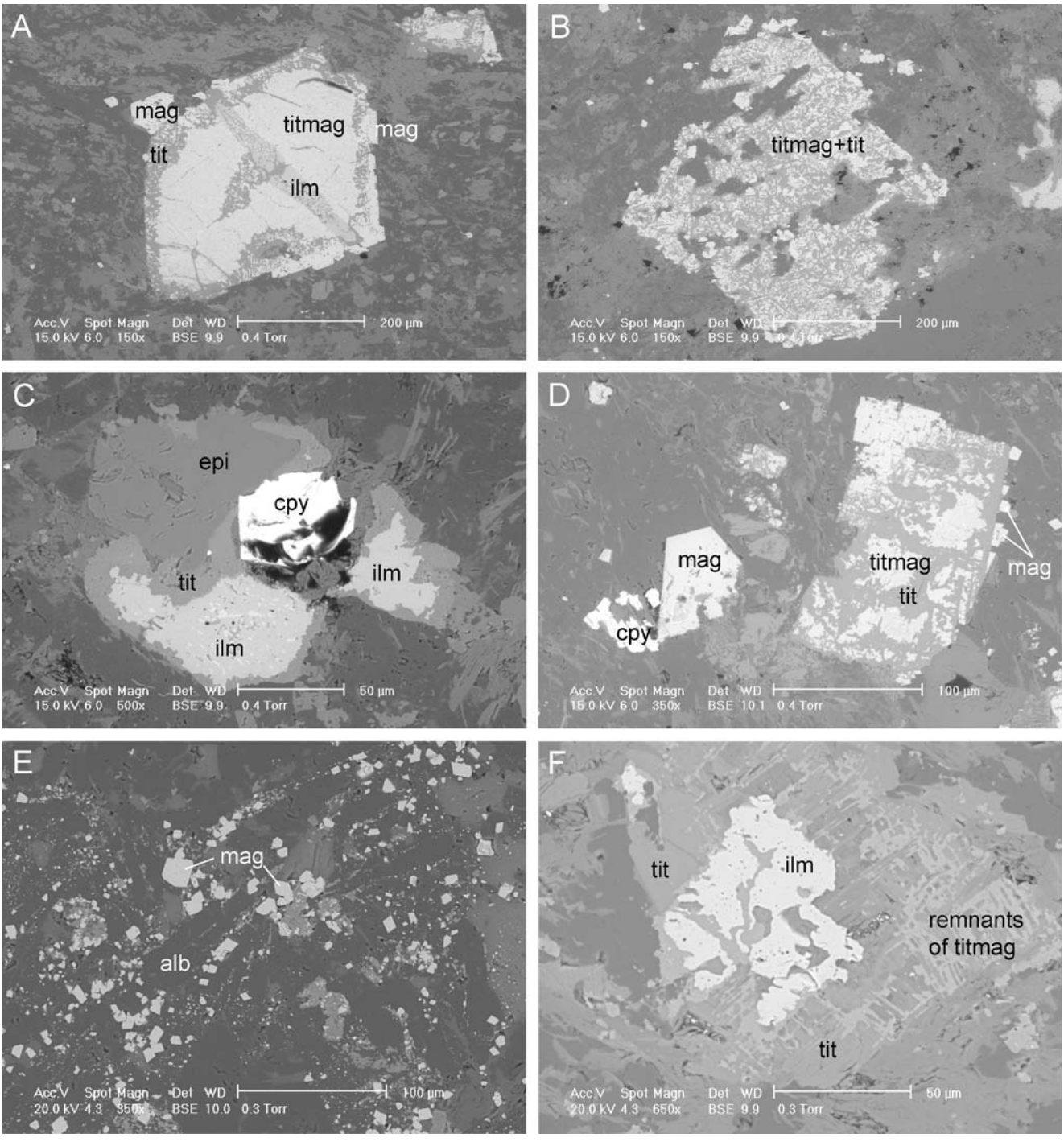

Fig. 4 **a**–**f** Back-scattered electron images of iron–titanium oxides and sulphides from metabasalt samples from the mine area. **a** Albite–actinolite alteration of coarse-grained metabasalt—titanomagnetite crystal with central lamellae of ilmenite and minor titanite alteration. Magnetite occurs as fine-grained euhedral crystals and as overgrowths on titanomagnetite. **b** Albite–actinolite alteration of fine-grained metabasalt—titanomagnetite crystal with fine exsolution lamellae. Titanium-rich lamellae are altered to titanite (*dark grey*). **c** Albite–actinolite alteration—interstitial chalcopyrite between epidote and ilmenite. The ilmenite crystal is rimmed by titanite. **d** Calcite–magnetite alteration—titanomagnetite crystal with titanite alteration along titanium-rich exsolution lamellae. Magnetite occurs as euhedral crystals and as fine-grained crystals rimming the titanomagnetite. Chalcopyrite is also present. **e** Calcite–magnetite alteration—hydrothermal breccia-clusters of magnetite crystals with a groundmass of albite laths in a breccia clast. **f** Biotite–ilmenite alteration—ilmenite crystal overprinting titanite that preserves texture of pre-existing titanomagnetite. Abbreviations for Figs. 4 and 5: *alb* albite, *bio* biotite, *cal* calcite, *chl* chlorite, *cpy* chalcopyrite, *epi* epidote, *hbl* hornblende, *ilm* ilmenite, *kfs* K-feldspar, *mag* magnetite, *qtz* quartz, *tit* titanite, *titmag* titanomagnetite

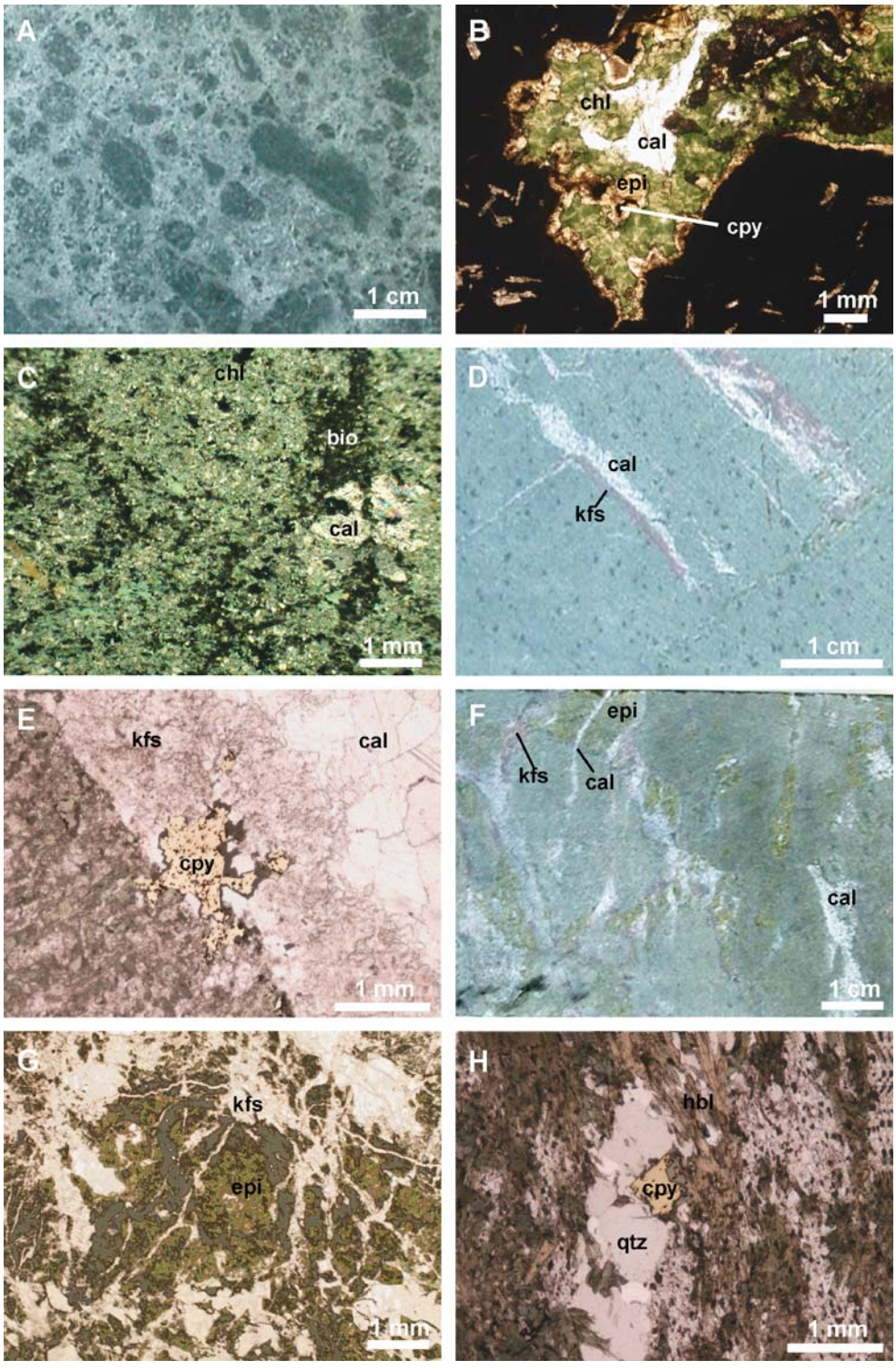

Fig. 5 **a** Hydrothermal breccia with intense calcite–magnetite alteration. Clasts consist of clots of magnetite. **b** Vesicle in the Cromwell Metabasalt lined within epidote intergrown with chalcopyrite, then chlorite and then calcite. **c** Fine biotite veinlets overprinting foliated metabasalt with calcite. **d** Albite–actinolite-altered Cromwell Metabasalt with titanomagnetite crystals overprinted by K-feldspar–calcite–chalcopyrite veins. **e** K-feldspar–calcite–chalcopyrite vein cutting Cromwell Metabasalt. **f** Intense epidote metasomatism of the Cromwell Metabasalt, which was cut by K-feldspar–calcite veins. **g** Intense K-feldspar veining overprinting epidote. **h** Amphibolite with quartz–chalcopyrite vein overprinted by hornblende from the Hazeldene area. Abbreviations in Fig. 4 caption

In the albite–actinolite- and calcite–magnetite-altered metabasalts, K-feldspar–calcite–chalcopyrite veins cut the regional S_2 foliation. The vein boundaries are sharp and not overgrown by other minerals, suggesting a post-metamorphic timing (Fig. 5e). These veins contain only minor chalcopyrite when they overprint zones of epidote alteration and veining (Fig. 5f,g). In some cases, euhedral magnetite occurs within quartz–calcite–K-feldspar veins. Northwest of the mine area, K-feldspar-filled vesicles are prominent in metabasalts. In these examples, K-feldspar has overprinted or enclosed epidote in the vesicles.

Hazeldene area

Amphibolites

Amphibolites from the Hazeldene area, west of the Mount Isa Fault, are geochemically equivalent to metabasalts in lower metamorphic grade rocks elsewhere and are dominated by coarse-grained hornblende and interstitial fine-grained, interlocking sodic plagioclase and quartz (consistent with the findings of Rubenach 1992). Twinned plagioclase laths are rarely preserved. The hornblende crystals are aligned parallel to the S_2 regional foliation. The samples can be divided into coarse-, medium- and fine-grained amphibolites based on the relative size of the hornblende crystals. In the coarse-grained amphibolites, titanomagnetite–ilmenite intergrowths are preserved, as they were in the coarse-grained metabasalt samples from mine section 38,000 mN. In medium-grained amphibolites, coarse-grained intergrowths of magnetite and ilmenite occur. In fine-grained samples, the iron oxides have recrystallised to coarse-grained euhedral magnetite and to fine-grained rods of ilmenite throughout the groundmass.

The amphibolites from the Hazeldene area contain two dominant vein types: quartz–chalcopyrite and epidote–quartz. Quartz–chalcopyrite veins are overprinted by hornblende (Fig. 5h), and epidote–quartz veins are boudinaged and oriented parallel to the regional S_2 foliation, as defined by the hornblende, suggesting an early syn-metamorphic timing for both.

Mineral chemistry

Analytical techniques

Polished blocks of each sample were prepared for in situ geochemical analysis of iron–titanium oxides in the metabasalts. Major element chemistry (Table 2) was determined using a Cameca SX-50 electron microprobe housed at the University of Melbourne. The electron gun was operated at an acceleration voltage of 15 kV and beam current of 25 nA for all analyses. Counting times were 20 s for all elements except V, which was counted for 60 s due to its low natural abundances in the oxides. The data were normalised to 100% in Table 2 for comparative purposes. The measured totals were 94.5–96.7% for titanomagnetite, 92.7–94.2% for magnetite, 96.6–100.5% for ilmenite and 95.5–98.8% for rutile.

Trace element concentrations were determined via laser ablation inductively coupled mass spectrometry (ICP-MS) to remove the effects of mineral inclusions in the iron–titanium oxides. The data were obtained using a Finnigan MAT Element ICP-MS coupled with a Merchantek LUV 266 nm Nd:YAG laser at Monash University. Analyses employed a pulse rate of 4 Hz and a beam energy of 1 mJ, producing a spot size of approximately 50 μm. For each analysis (mass cycle), background readings were collected for 10 s before beginning ablation for 50 s. The ICP-MS was purged for 15 s between each analysis.

Table 2 Average microprobe data for iron–titanium minerals normalised to 100 wt%

Mine area													Hazeldene area							
Sample	MG02027	MG02015	MG02027	MG02015	MG02039	MG02017	MG02027	MG02041	MG02048	MG02049	MG02049	MG02050	MG03029	MG03029	MG03031	MG03033	MG03029	MG03031	MG03033
Description	cg alb–act	cal–mag	alb–act	cal–mag	bc cal–mag	epi–tit	alb–act	alb–act	bio–ilm	bio–ilm	bio–ilm	chl–rut	cg amph	cg amph	mg amph	fg amph	cg amph	mg amph	fg amph
Mineral (*n*)	titmag (4)	titmag (3)	mag (3)	mag (6)	mag (5)	mag (5)	ilm (2)	ilm (3)	ilm (2)	ilm (4)	rutile (2)	rutile (3)	titmag (3)	mag (1)	mag (7)	mag (5)	ilm (1)	ilm (6)	ilm (5)
SiO_2	0.37	0.13	0.85	1.20	0.21	N.D.	N.D.	N.D.	0.19	1.05	3.45	1.36	0.83	0.16	N.D.	N.D.	N.D.	N.D.	0.36
TiO_2	24.14	22.68	0.24	0.24	0.17	N.D.	52.40	51.48	51.98	50.80	91.72	88.27	16.61	2.11	N.D.	N.D.	51.48	50.99	50.10
Cr_2O_3	0.18	N.D.	0.12	0.13	N.D.	N.D.	N.D.	N.D.	N.D.	N.D.	N.D.	N.D.	N.D.	N.D.	N.D.	N.D.	N.D.	N.D.	N.D.
Al_2O_3	N.D.	N.D.	0.29	N.D.	N.D.	N.D.	N.D.	N.D.	N.D.	0.58	0.64	0.90	0.20	N.D.	0.14	0.24	N.D.	N.D.	0.15
V_2O_3	1.87	1.32	1.47	1.16	0.68	0.61	0.34	0.37	N.D.	N.D.	0.51	0.54	0.46	0.96	0.97	0.62	0.31	N.D.	N.D.
FeO	69.85	72.83	96.69	97.13	98.79	99.39	38.86	42.32	43.64	41.22	1.31	1.46	80.71	96.78	98.89	99.14	46.05	47.36	46.74
MnO	3.23	2.91	N.D.	N.D.	N.D.	N.D.	8.22	5.71	4.00	3.14	N.D.	N.D.	0.63	N.D.	N.D.	N.D.	2.16	1.49	1.60
MgO	N.D.	N.D.	0.22	N.D.	N.D.	N.D.	N.D.	N.D.	N.D.	0.48	0.59	0.88	0.12	N.D.	N.D.	N.D.	N.D.	0.16	0.45
CaO	0.36	0.13	0.11	0.15	0.14	N.D.	0.19	0.12	0.18	2.73	1.78	6.58	0.45	N.D.	N.D.	N.D.	N.D.	N.D.	0.59

titmag titanomagnetite, *mag* magnetite, *ilm* ilmenite, *n* number of analyses, *N.D.* not detected, *cg* coarse-grained, *mg* medium-grained, *fg* fine-grained, *amph* amphibolite, *bc* breccia, *alb–act* albite–actinolite, *cal–mag* calcite–magnetite, *epi–tit* epidote–titanite, *bio–ilm* biotite–ilmenite, *chl–rut* chlorite–rutile

The laser ablation ICP-MS data were reduced using the software GLITTER 4.0 (van Achterbergh et al. 2001). Quantitative results for 15 elements were obtained through calibration of relative element sensitivities using the NIST 610 or NIST 612 glass as an external standard (Table 3). Electron microprobe data for Ti, V or Fe were used for internal standardisation (all data can be found in ESM 1 Appendix 1). Iron was found to be a very poor internal standard due to the large mass overlap between ^{57}Fe and ArOH (from the Ar carrier gas) and was avoided wherever possible. Detection limits were typically less than 10 ppm for the majority of elements but may reach tens of parts per million for Ti, Ni, Mn, As and Cr and hundreds of parts per million for Fe, where the instrument background level is high due to ArOH mass overlap.

Over 100 mineral grains were analysed, but those analyses that represented a mixture of more than one mineral were discarded to create a high-quality dataset for interpretation. The GLITTER software allows the user to select the portion of the analytical spectra used for quantification. Each spectrum was inspected for any evidence indicative of mineral inclusions. The portion of the spectra used for quantification was selected where the spectra was flat, excluding the first part of the ablation where the signal contained interferences from sample surface effects. A minimum of 10 s of spectra was used from each analysis to ensure that results were representative of the sample.

The spot size was typically equivalent to the dimensions of oxide grains, allowing only one analysis per grain. Therefore, there is no discussion of the intragrain variability, and analyses represent an average of the grains. The averages and standard deviations calculated for each sample (Table 3) suggest variability between grains. For samples in the mine area, one standard deviation around the average for Cu, Co and Ni ranged between 15 and 30% of the average, which was independent of mineral phase. For samples in the Hazeldene area, concentrations were more variable, with one standard deviation representing up to 23% of the average for Co and 38% for Ni. However, copper showed the most variability between grains, one standard deviation representing up to 103% of the average.

The NIST 612 standard glass was analysed as an unknown twice for every ten mineral analyses to assess the quality of the data. A comparison of the results for the unknown NIST 612 using Ti and V as the internal standard is shown in ESM 2 Appendix 2 and compared well with the reported values of Pearce et al. (1997).

Iron–titanium oxide chemistry

Titanomagnetite occurs in albite–actinolite- and calcite–magnetite-dominated rocks from the mine area and in coarse-grained amphibolites from the Hazeldene area. Major element geochemistry of various titanomagnetites shows minor differences (Table 2). Titanomagnetites from the mine area contain approximately 10% less iron, 7% more titanium and 2.5% more manganese than those in the Hazeldene area, resulting in the mine examples being higher in ferrous iron (Fe^{2+}), when the microprobe data are recalculated on the basis of four oxygen atoms. The Cu content of titanomagnetite varies between 18 and 40 ppm (Table 3), which correlates with the amount of ferrous iron

Table 3 Average LA-ICP-MS data for iron–titanium minerals (parts per million)

Mine area													Hazeldene area							
Sample	MG02027		MG02015		MG02015		MG02039		MG02017		MG02050		MG03029		MG03031		MG03033		MG03031	
Description	cg alb–act		cal–mag		cal–mag		bc cal–mag		epi–tit		chl–rut		cg amph		mg amph		fg amph		mg amph	
Mineral (*n*)	titmag (6)		titmag (4)		mag (3)		mag (2)		mag (5)		ilm (4)		titmag (4)		mag (2)		mag (4)		ilm (3)	
	ave.	s.d.	ave.	s.d.	ave.	s.d.	ave.	s.d.	ave.	s.d.	ave.	s.d.	ave.	s.d.	ave.	s.d.	ave.	s.d.	ave.	s.d.
Sc	6.43	4.29	20.3	6.86	2.91	0.16	100	7.86	2.06	1.00	138	18.6	10.5	13.5	3.61	2.58	1.17	0.77	31.6	21.4
Cr	785	242	681	572	247	162	690	56.4	133	101	384	290	69.8	29.1	1222	334	327.	71.6	15.6	8.48
Co	21.5	6.48	22.9	4.75	14.4	4.43	358	7.10	40.9	6.79	44.4	10.9	54.4	12.6	175	21.0	87.4	2.10	129	1.85
Ni	25.3	4.45	17.8	2.44	18.5	5.84	816	14.3	61.8	7.07	264	64.4	42.9	16.3	170	19.9	124	3.09	33.5	12.1
Cu	39.2	22.4	28.5	6.40	8.91	1.22	1.93	0.59	2.71	0.59	3.69	1.08	18.8	19.4	72.7	43.4	32.7	32.4	122	21.5
Zn	77.2	26.7	86.7	29.6	16.8	5.15	725	24.2	34.1	11.7	383	90.0	83.2	11.0	101	19.2	54.8	25.8	250	19.0
Ge	2.61	1.08	4.28	2.10	0.95	0.05	N.D.		6.55	1.98	6.00	1.33	2.01	0.36	6.42	3.54	3.07	0.54	N.D.	
As	16.9	4.25	19.9	1.99	2.88	1.21	36.8	30.5	6.14	0.89	N.D.		12.6	3.68	29.8	7.91	82.8	3.54	16.9	0.81
Nb	60.3	25.4	56.9	21.9	3.38	0.14	10.2	6.94	1.64	2.79	295	42.1	77.0	1.86	0.13	0.03	0.49	0.41	247	2.44
Sn	3.18	1.73	5.56	3.09	1.00	0.17	3.70	0.97	2.37	1.86	58.2	6.21	0.88	0.35	3.32	2.88	N.D.		5.43	6.19
Sb	2.61	0.44	3.35	0.49	0.69	0.34	1.13	0.43	0.29	0.07	6.95	0.77	0.82	0.35	N.D.		N.D.		0.54	0.30
W	1.93	0.92	2.45	0.50	0.32	0.10	0.98	0.80	0.40	0.41	26.3	2.76	1.07	0.20	0.86	1.07	0.36	0.36	3.67	0.60
Tl	0.02	0.01	0.01	0.01	0.03	0.02	0.46	0.04	0.63	1.08	0.26	0.11	0.07	0.04	0.03	0.03	0.02	0.02	0.02	0.00
Pb	10.6	2.13	9.69	3.78	2.16	0.96	5.15	0.20	2.42	1.27	13.2	1.64	1.78	2.02	1.20	0.20	1.28	0.90	3.54	0.64
Bi	0.26	0.12	0.62	0.27	0.06	0.05	0.06	0.02	0.03	0.02	0.06	0.04	0.03	0.02	0.15	0.15	0.02	0.01	0.14	0.11

Abbreviations as in Table 2
ave. average, *s.d.* standard deviation

in the host mineral. Copper as Cu^{2+} will substitute for Fe^{2+} (Goldschmidt 1954); therefore, the relatively higher ferrous iron titanomagnetites from the mine area are higher in Cu. This correlation would not occur if sulphide inclusions in the titanomagnetite were controlling the Cu content.

Magnetite typically occurs in albite–actinolite, calcite–magnetite and some epidote–titanite assemblages and amphibolites. In terms of major elements, the magnetites are all geochemically very pure (Table 2). The Cu content of magnetite varies between 1 and 9 ppm in the mine area samples, which is significantly lower than magnetites from the Hazeldene area, which range from 32 to 73 ppm Cu (Table 3). Even when the large standard deviations found in the Hazeldene samples are taken into account, the two populations are statistically distinct.

Plots of Cu against Ni/Cr and Cu against Co/Ni for titanomagnetite and magnetite from the mine area reveal two separate populations (Fig. 6a,b). Titanomagnetites have high Cu at low Ni/Cr and high Co/Ni ratios. Magnetites have low Cu at variable but high Ni/Cr and low Co/Ni ratios. The opposite trend is found for titanomagnetite and magnetite in amphibolite samples from the Hazeldene area, where magnetite contains higher concentrations of Cu at lower Co/Ni ratios compared with titanomagnetites (Fig. 6c).

Ilmenite is present in albite–actinolite and biotite–ilmenite assemblages, as well as in amphibolites from the Hazeldene area. Albite–actinolite-associated ilmenite is characterised by traces of vanadium and significant manganese up to 8.22 wt% MnO. Ilmenite associated with biotite has moderate manganese contents (up to 4.00 wt% MnO), and Hazeldene ilmenite contains low concentrations of manganese (up to 2.16 wt% MnO; Table 2). The MnO content of ilmenite decreases with increasing metamorphic grade, consistent with studies of ilmenite in other metamorphic terranes (Cassidy et al. 1988).

The Cu content of ilmenite appears to vary significantly with the alteration type (although this observation is based on limited data). Ilmenite from the Hazeldene area contains the most elevated Cu concentrations of up to 122 ppm Cu (Table 3). In comparison, ilmenites associated with biotite alteration from the mine area contain almost no Cu (less than 4 ppm).

Geochemical modelling

Copper mobility in the Eastern Creek Volcanics during metamorphism was modelled using the software Geochemist's Workbench (Bethke 1998) with the Unitherm thermodynamic dataset (Shvarov and Bastrakov 1999). The Unitherm dataset was chosen due to its superior thermodynamic data for epidote and chlorite, which are important in this modelling scenario. The first step was to equilibrate a fluid with a metabasalt, characterised texturally as weakly calcite–magnetite-altered, using appropriate mineralogy obtained by X-ray diffraction analysis (Table 4). This simulation was designed to represent greenschist facies

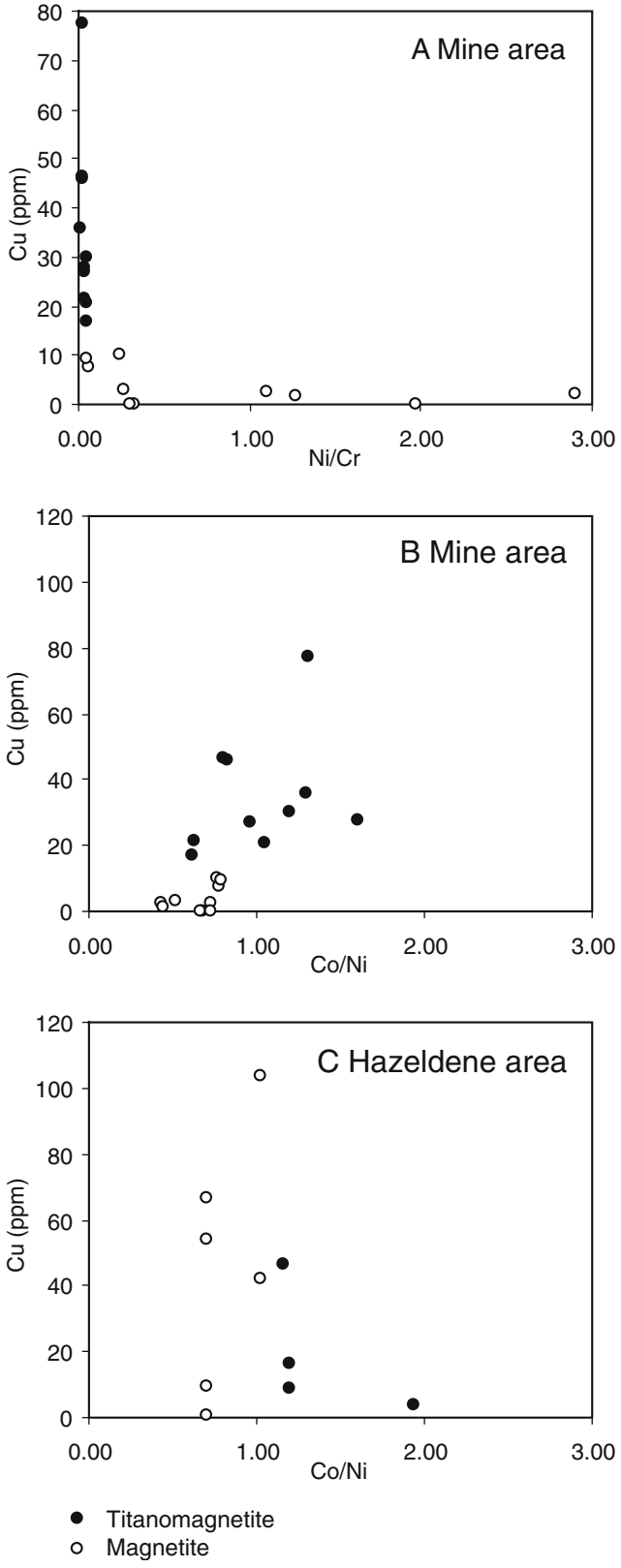

Fig. 6 **a**–**c** Bivariate plots using laser ablation ICP-MS data for titanomagnetite and magnetite. **a** Cu vs Ni/Cr comparing titanomagnetite and magnetite from the mine area. **b** Cu vs Co/Ni comparing titanomagnetite and magnetite from the mine area. **c** Cu vs Co/Ni comparing titanomagnetite and magnetite from the Hazeldene area. All data in Appendix 1

Table 4 Geochemical modelling data

Input data	
Condition	Value
T	250°C
P	50 MPa
$fO_{2(g)}$	−40
$fCO_{2(g)}$	−5
Input rock	Weight (g)
Albite	145
Anorthite	145
Calcite	15.5
Chlorite	284
Epidote	59.5
Magnetite	58
Microcline	94.5
Quartz	196
Chalcopyrite	2.5

metamorphism with CO_2 input from the adjacent sedimentary rocks at 250°C and 50 MPa. A temperature of 250°C was chosen to reflect the lower greenschist facies conditions represented by mineral assemblages at Mount Isa as indicated by illite crystallinity measurements in the Urquhart Shale (Gregory 2005). The Urquhart Shale samples used in this estimate were from outside the influence of copper mineralisation, as the mineralising event may have imparted a higher temperature overprint. A pressure of 50 MPa is lower than the predicted pressure conditions during regional metamorphism at Mount Isa; however, the pressure conditions were found to have little influence on the modelling scenarios undertaken by Heinrich et al. (1995).

The copper content of the fluid phase increased as the model proceeded due to the progressive breakdown of chalcopyrite (Fig. 7a). Textural and geochemical data indicate that titanomagnetite is breaking down and forming magnetite during the same process, with copper released into the fluid phase. The absence of thermodynamic data for titanium phases, such as titanomagnetite, precludes this transformation from the modelling experiments. However, the most important aspect is that if copper is released from the titanomagnetites, then it can be carried by the fluid produced in equilibrium with the metabasalts, which is consistent with this modelling.

The same modelling experiment using a calcite-poor metabasalt did not produce a fluid with significant copper as chalcopyrite, and from textural evidence titanomagnetite, remained stable.

The second part of the modelling process was to take the copper-bearing output fluid from the first step and flush it through the same rock at increasing fluid–rock ratios to model the migration of metamorphic fluids into zones of high permeability, i.e. metasomatism. The results show that with increasing amounts of fluid, the mineralogy of the rock becomes dominated by epidote, quartz and chlorite at the expense of albite, K-feldspar, calcite and iron oxides (Fig. 7b). Chalcopyrite precipitation occurs where epidote

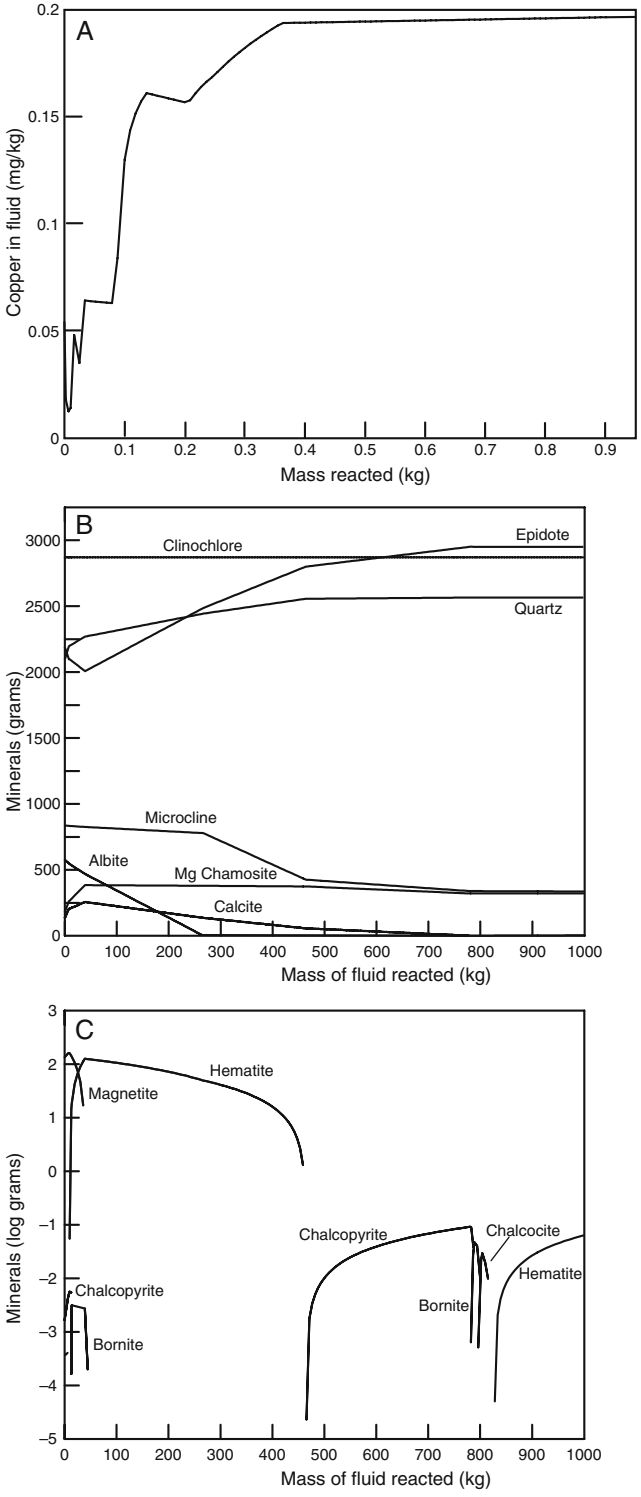

Fig. 7 **a**–**c** Geochemical modelling results. **a** Concentration of copper in a fluid in equilibrium with Cromwell Metabasalt (mineralogy defined by XRD) at 250°C and 50 MPa. **b** Change in silicate mineralogy as the fluid from (**a**) is flushed through the same metabasalt in increasing volumes at 250°C and 50 MPa. **c** Oxide and sulphide mineral assemblage resulting during (**b**). Note that chalcopyrite is stabilised where epidote dominates the assemblage at high fluid–rocks ratios. Input data in Table 4

dominates the assemblage at high fluid–rock ratios (470:1 to 800:1) (Fig. 7c). At very high fluid–rock ratios (greater than 800:1), chalcopyrite becomes unstable again.

Regional geochemistry

All available analytical data for the Eastern Creek Volcanics were collated from the OZCHEM database (Geoscience Australia) and Xstrata Copper (unpublished data). The resulting whole rock analyses have been divided into areas for comparison of regional geochemistry. The average copper content of metabasalts in the Gunpowder area is considered to be the closest possible approximation to the original magmatic copper content of the Eastern Creek Volcanics (Wilson et al. 1985; Gregory et al., in preparation). Using the data collated in the current study for metabasalts from the Gunpowder area, the Cromwell Metabasalt Member has an average copper content of 201 ppm, and the Pickwick Metabasalt Member has an average of 153 ppm. These average values compared closely with the published averages of Wilson et al. (1985) and Hannan et al. (1993).

The copper content of metabasalts in the Gunpowder area is well above the averages for samples from the Haslingden and Hazeldene areas (Table 5). The lower values in the Haslingden and Hazeldene areas are in part due to a mass increase in these rocks due to metamorphism and hydrothermal alteration. Using the isocon method (Grant 1986) and average whole-rock analyses, each of the three areas can be compared directly. The isocon lines were chosen based on a line of best fit through all elements, except those which are obviously mobile during metamorphism and potassic alteration (K_2O, Rb, Li and Cu). This is based on the guidelines of Grant (1986) who suggested that it was best to choose an isocon based on as many geochemically different species as possible. This is different from the isocons defined by Hannan et al. (1993) and Heinrich et al. (1995) who used the traditional immobile elements of Al, Nb, Y, Zr, Ti and P. The method employed in the current study is considered more robust as Wyborn (1987) found anomalous Zr and Y concentrations in epidote–titanite- and calcite–magnetite-altered metabasalts, suggesting that these elements were not immobile. As the current study is concerned with the effects of epidote–titanite alteration, it is not desirable to solely constrain the isocons with elements which are important in epidote alteration such as Al_2O_3.

From the graphical display of the data in Fig. 8, it is clear that Al_2O_3, Nb, Y, TiO_2 and P_2O_5 do not lie in a linear array through the origin, thereby justifying the use of other elements for isocon construction. However, in Fig. 8a, the traditional immobile elements lie very close to the calculated isocon, and overall, there is a narrow spread in

Table 5 Average copper content of Eastern Creek Volcanics

Area	Metabasalt member (*n*)	Cu (ppm)	Mass change[a] (%)
Gunpowder	Cromwell Metabasalt (46)	201	–
	Pickwick Metabasalt (11)	153	–
Haslingden	Cromwell Metabasalt (96)	145	12
	Pickwick Metabasalt (40)	118	−1
	Cromwell Metabasalt Epidosite (13)	188	24
Hazeldene	Pickwick Metabasalt (61)	99	−6

[a]Mass change calculated using the Grant isocon method (Grant 1986)

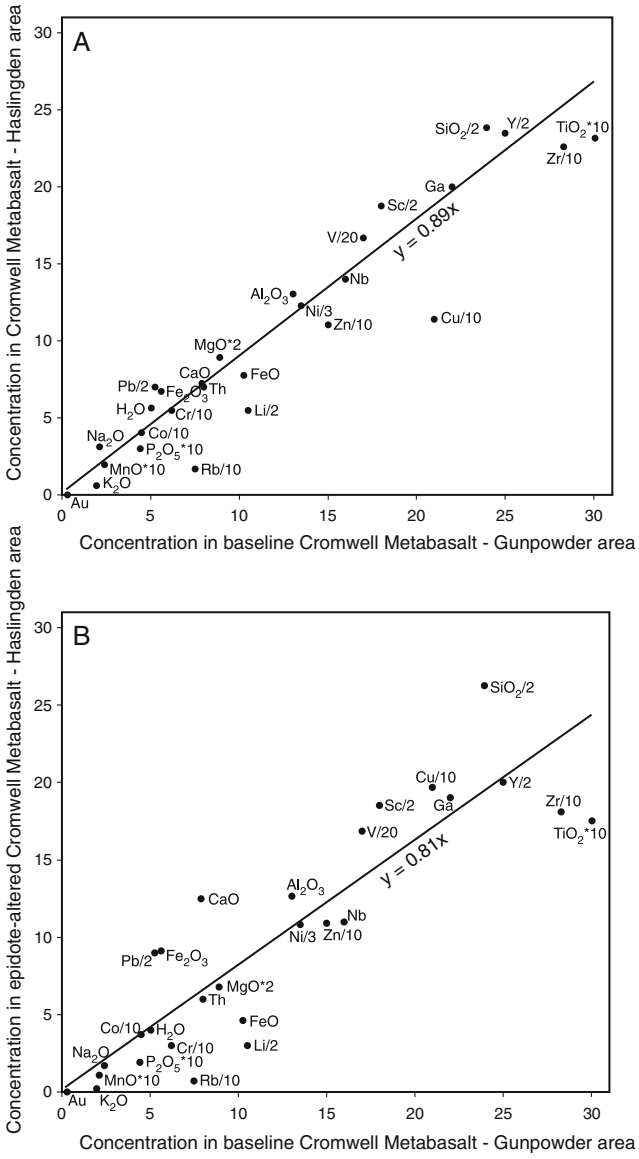

Fig. 8 a, **b** Grant (1986) isocon plots of median element concentrations in Cromwell Metabasalts from the Gunpowder area plotted against: **a** Cromwell Metabasalts from the Haslingden area (excluding epidote-altered samples) and **b** epidote-altered Cromwell Metabasalts from the Haslingden area. The gradient of the lines of best fit (mobile elements K_2O, Rb, Li and Cu excluded) were used to calculate the gains and losses in Table 5. All data are sourced from the OZCHEM database (Geoscience Australia) and Xstrata Copper (unpublished); number of samples used to define average metabasalt compositions are listed in Table 5

the data, suggesting that either method of isocon construction discussed above would produce the same results in this example. Both Ni and Co lie precisely on the isocon line in this example.

Figure 8b displays a wide spread in the data; however, the isocon line of best fit still passes through Ni and Co. The elements which are the main constituents of epidote (Al, Fe, Ca, Si) all plot to the left of the isocon, indicating that they are enriched relative to the majority of other elements and justifying the use of a wider array of elements in isocon construction. The results contrast with the findings of Hannan et al. (1993) who interpreted that epidote alteration occurred without volume change or significant change in Al_2O_3 concentrations based partly on the assumption that Al_2O_3 was immobile.

The most significant results are found when comparing the average Cromwell Metabasalt from the Gunpowder area with average Cromwell Metabasalt in the Haslingden area. There is a significant loss of K_2O, Rb, Li, TiO_2 and Cu in Haslingden area Cromwell Metabasalt (Fig. 8a). The same elemental losses are found when epidote-altered metabasalts from the Haslingden area are compared with the more pristine metabasalts from the Gunpowder area with the exception of Cu, which is gained in epidote-altered samples (Fig. 8b).

The relative geochemical differences can be compared spatially by interpolating the data using the inverse distance squared method. Variations in CaO directly reflect the metabasalt mineralogy, with highs in the eastern Haslingden area representing epidote enrichment and highs in the western Hazeldene area representing hornblende growth (Fig. 9a). There is a general correlation between elevated CaO and elevated Cu in the Haslingden area, although there are some sub-areas of low Cu within the overall high-Cu region (Fig. 9b). The distribution of K_2O is concentrated in the northeast of the Haslingden area, and there is very strong enrichment along northwest–southeast zones in this area, which most likely correlate with major faults (Fig. 9c). The strong enrichment in K_2O correlates with areas of low Cu, and a plot of K_2O/Cu highlights these areas in the Haslingden area (Fig. 9d).

Table 6 shows an analysis of the geochemical dataset with respect to potassic and epidote alteration in both the Haslingden and Hazeldene areas. Potassic-altered metabasalts have significantly lower Cu concentrations compared with the unaltered (low K_2O) equivalent metabasalts. The sample population without potassic alteration contains Cu concentrations consistent with the baseline Gunpowder values once the mass increase due to alteration is taken into account (Table 5). In the Haslingden area, metabasalts can be divided into epidote-rich, characterised by high CaO and Fe_2O_3 contents, and epidote-poor samples. Epidote-rich samples contain elevated Cu concentrations compared with the regional average, whilst metabasalts without epidote or potassic alteration (albite–actinolite- or calcite–magnetite-dominated samples) contain lower Cu concentrations (Table 6).

Discussion

Timing and genesis of iron–titanium oxides

The occurrence and texture of titanomagnetite suggest that it is a remnant magmatic phase within the metabasalts in the mine area. Observations made in this study suggest that titanomagnetite is typically preserved in albite–actinolite assemblages and breaks down during regional peak metamorphism, with the stable oxide assemblage under greenschist facies conditions identified as magnetite and titanite. Calcite–magnetite-bearing assemblages are dominated by the growth of new metamorphic magnetite in place of titanomagnetite. This relationship may indicate that the presence of CO_2 accelerates this transformation. Epidote–titanite assemblages have resulted from the complete breakdown of titanomagnetite with extensive titanite development. The lack of magnetite is attributed to the growth of Fe-rich epidote, which has incorporated the majority of the available iron. In the amphibolites of the Hazeldene area, titanomagnetite is only preserved in coarse-grained samples, whilst magnetite dominates in fine-grained examples, suggesting that coarse-grained metabasalts are slower to recrystallise during regional metamorphism.

The Co/Ni ratios in magnetite and titanomagnetite reflect the genesis of the phase. A Co/Ni ratio above 1 suggests a higher temperature, igneous origin for magnetite, whereas ratios less than 1 indicate a relatively low temperature, metamorphic hydrothermal or sedimentary genesis (Frietsch 1970). Titanomagnetites and magnetites from the Eastern Creek Volcanics preserve variable Co/Ni ratios (Fig. 6b,c). Titanomagnetites have the highest Co/Ni ratios, the majority of which are above 1, supporting a primary magmatic origin. The Co/Ni ratios of the magnetites reflect the low- or high-grade metamorphic environment under which they formed. Magnetites in amphibolites from the Hazeldene area have ratios between 0.70 and 1.03 compared with samples from the lower metamorphic grade mine area which have lower ratios of 0.44 to 0.79, consistent with the lower temperatures that were experienced during formation (cf. Fig. 6b with c).

The petrology and mineral chemistry presented in this study support the proposed framework of magmatic titanomagnetite, which is preserved in albite–actinolite greenschist facies assemblages and coarse-grained amphibolites, and metamorphic magnetite in calcite–magnetite assemblages and fine-grained amphibolites.

Copper mobility during regional metamorphism

The lack of magmatic sulphide formation during fractionation and crystallisation of the Eastern Creek Volcanic magma has resulted in oxide phases hosting significant copper concentrations (Gregory et al., in preparation). The copper content of titanomagnetite varies between an average of 34.9 ppm in the mine area and 18.8 ppm in the Hazeldene area. Copper released from titanomagnetite

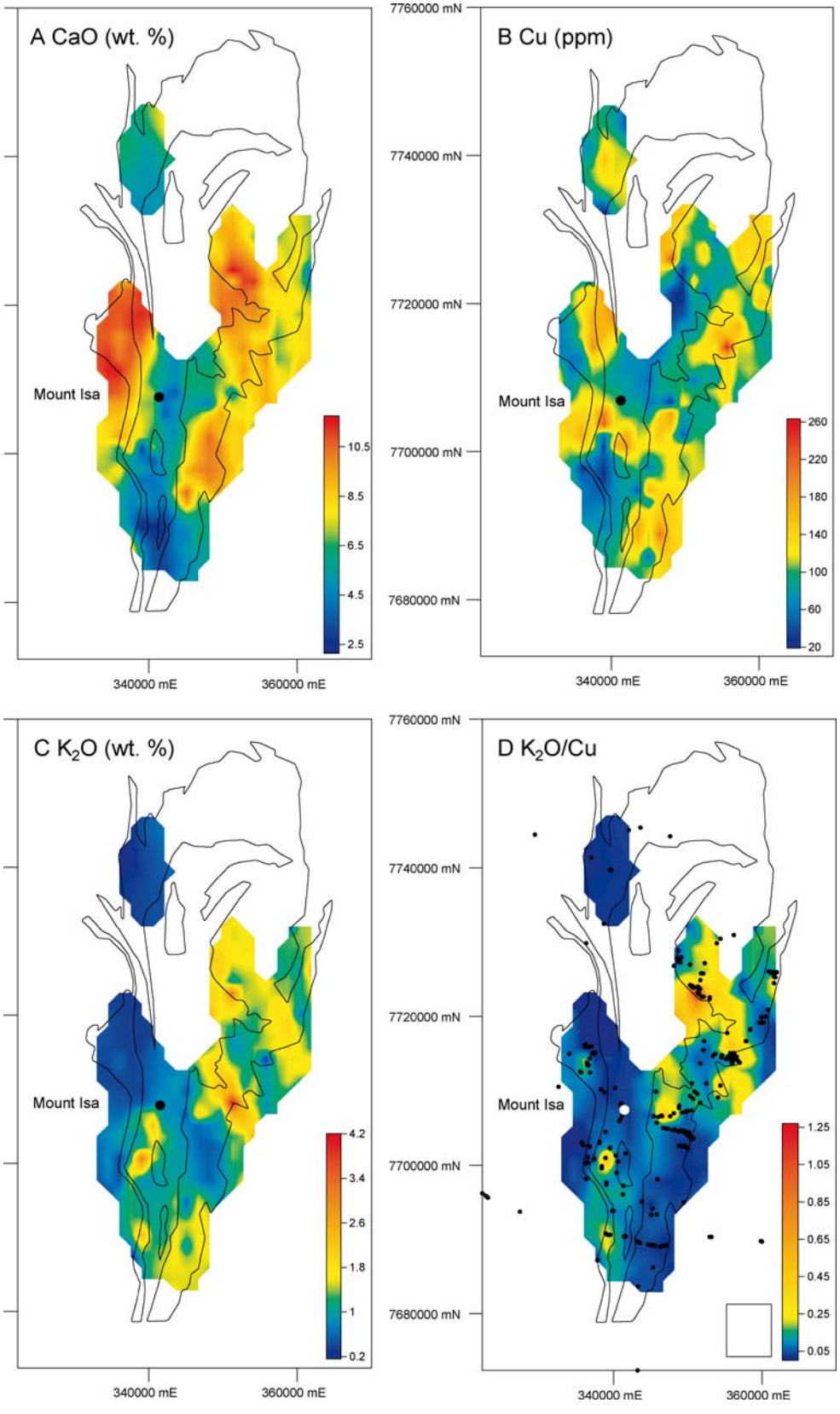

Fig. 9 **a**–**d** Inverse distance squared interpolation of Eastern Creek Volcanics geochemical data from the OZCHEM database (Geoscience Australia) and Xstrata Copper (unpublished). **a** CaO (weight percent). **b** Cu (parts per million). **c** K_2O (weight percent). **d** K_2O/Cu. *Black points* show sample locations. Interpolation uses a north–south-orientated, 8×4-km search ellipse. Data are overlain by an outline of the surface extent of the Eastern Creek Volcanics. *Rectangle* on plot (**d**) represents area needed to be leached of Cu to account for Mount Isa copper deposit

during lower greenschist facies metamorphism in the mine area has not been incorporated into metamorphic magnetite (Fig. 6b). This is in contrast to samples from the Hazeldene area where metamorphic magnetite accumulated copper not just from the breakdown of titanomagnetite but also presumably from the breakdown of other copper-bearing phases (Fig. 6c). Magmatic/metamorphic ilmenite from the Hazeldene area contains the highest copper content of all

Table 6 Average copper contents for potassic and epidote-altered metabasalts from the Haslingden and Hazeldene areas

All metabasalts	Potassic alteration	Epidote alteration
Haslingden area; Cromwell Metabasalt dominates area. 123 ppm Cu, *n*=267	Low K_2O (0.71 wt%), 164 ppm Cu, *n*=168	Epidote poor[a], 142 ppm Cu, 5.09 wt% CaO, 5.32 wt% Fe_2O_3, *n*=40 Epidote rich, 171 ppm Cu, 9.56 wt% CaO, 9.41 wt% Fe_2O_3, *n*=128
	High K_2O (2.09 wt%), 52 ppm Cu, *n*=99	
Hazeldene area; Pickwick Metabasalt dominates area. 99 ppm Cu, *n*=61	Low K_2O (0.45 wt%), 147 ppm Cu, *n*=39	Not present
	High K_2O (1.57 wt%), 14 ppm Cu, *n*=22	

[a]Epidote-poor samples are characterised by albite–actinolite- or calcite–magnetite-altered metabasalts.

the iron–titanium oxides analysed, with an average of 122 ppm Cu. This suggests that copper was redistributed between iron–titanium oxides in the Hazeldene area, whereas it was mobilised in the mine area.

In the mine area, the process by which titanomagnetite broke down to magnetite was associated with CO_2 addition and calcite precipitation in the metabasalts. Epidote growth was concurrent with titanomagnetite breakdown and magnetite growth, occurring across the peak of regional metamorphism. Epidote–chalcopyrite intergrowths are common, suggesting that copper mobilised by metamorphism was concentrated in areas rich in epidote.

Geochemical modelling demonstrated that copper can be remobilised from metabasalts during greenschist facies metamorphism and reprecipitated in zones of high permeability, which experience high fluid–rock ratios. An important factor was the presence of CO_2 which created the right pH conditions to enhance copper solubility. Copper solubility as a chloride complex is maximised under acidic conditions, and the presence of CO_2 may act as a weak acid which buffered the fluid composition. This means that the fluid could have maintained its elevated copper solubility in a similar manner in which gold is carried by CO_2-bearing metamorphic fluids in Archean greenstone belts (Phillips and Evans 2004). This process is consistent with the removal of copper from metabasalts during the transition from albite–actinolite assemblages that contain copper-rich titanomagnetite to calcite–magnetite altered rocks with copper-poor magnetite. Copper was released from the breakdown of magmatic titanomagnetite and chalcopyrite.

Geochemical modelling demonstrated that when the copper-bearing metamorphic fluid discussed above was channeled into zones of high permeability, such as faults, fractures and flow tops, epidote and quartz dominated the alteration. Magnetite became unstable and chalcopyrite became stable, explaining the close association of chalcopyrite and epidote. The modelling also suggested that at lower fluid–rock ratios, hematite was present in epidote-rich assemblages. Hematite has not been documented in epidote-rich assemblages in this study, but Bain et al. (1992) reported rare blades of hematite in intensely epidote-altered rocks in the Haslingden area. Fluid inclusion data from epidote-altered samples are $CaCl_2$ rich and CO_2 poor (Heinrich et al. 1995), indicating a loss of CO_2, probably due to calcite precipitation as part of calcite–magnetite alteration, and this loss of buffering capacity by the fluid may have contributed to the precipitation of chalcopyrite in epidote alteration zones. Fluid inclusion data for calcite–magnetite-altered rocks are not available for comparison.

A comparison of the regional geochemistry in the Haslingden area indicates that epidote-rich metabasalts contain higher copper concentrations compared with albite–actinolite or calcite–magnetite samples in the same area (Table 6). This distribution supports the idea that copper was locally remobilised from the metabasalts during regional metamorphism and concentrated in epidote alteration zones. This is in contrast to the findings of Hannan et al. (1993) who found mild copper depletion in epidote-altered metabasalts. However, the epidote-altered samples analysed by Hannan et al. (1993) were all collected from within the region where later potassic fluid-related copper depletion had occurred, and the reported depletion may reflect this process. They note that there is a large standard deviation on the average copper concentration in epidote-altered rocks due to anomalously depleted and high values which reflect the process identified in the current study. Epidote alteration is not a significant component of the Hazeldene area, and this is reflected in the fact that copper was redistributed between metamorphic iron-titanium oxide phases.

Copper depletion during potassic alteration

Biotite–ilmenite and chlorite–rutile assemblages are spatially related to the Paroo Fault and not the stratigraphy of the Eastern Creek Volcanics (Figs. 2 and 3). Biotite and ilmenite overprint chlorite, calcite and titanite and display a post-peak metamorphic timing. The alteration is spatially associated with chalcopyrite–pyrrhotite in the Mount Isa copper orebody above the Paroo Fault (Fig. 2). Previous research shows that the Mount Isa copper deposit also has a post-peak metamorphic timing (Perkins 1984; Swager 1985; Valenta 1994) similar to the timing of this biotite–

ilmenite and chlorite–rutile alteration. Isotopic dating of the copper ore suggests a Re–Os age of 1,377±59 Ma (Gregory et al., in review), which is consistent with Ar–Ar dating of biotite from biotite–ilmenite zones which gave an apparent age of between 1,352±3 and 1,385±3 Ma (Perkins et al. 1999).

K-feldspar–chalcopyrite veins consistently overprinted the albite–actinolite, calcite–magnetite and epidote–titanite assemblages and the metamorphic foliation (S_2). The late timing and potassic nature of this veining and replacement suggest a relationship to the biotite alteration found parallel to the Paroo Fault and associated with the Mount Isa copper deposit. The presence of chalcopyrite in the veins supports this interpretation and therefore, K-feldspar–calcite–chalcopyrite veins may represent the regional expression of copper mineralisation.

The regional geochemical dataset indicates a strong positive correlation between potassic-rich alteration and copper depletion most significantly in the Haslingden area and, to a lesser extent, in the Hazeldene area (Table 6). The potassium-rich zones in the metabasalts of the Haslingden area are only found within areas of epidote-altered metabasalts which are defined by elevated calcium (cf. Fig. 9a with c).

Previous work by Hannan et al. (1993) found elevated copper concentrations in biotite alteration in the Eastern Creek Volcanics at Lady Agnes. This biotite alteration was interpreted to be equivalent to biotite–ilmenite alteration below the Paroo Fault at Mount Isa. This is in contrast to this study where biotite-rich samples from Mount Isa are depleted in copper to a similar extent as chlorite–rutile-dominated metabasalts. The contrasting findings may reflect a greater extent of copper leaching at Mount Isa in comparison to Lady Agnes where significant copper mineralisation is absent.

The regional geochemical relationships between potassium and copper, together with the post-D_2 timing relationships for K-feldspar–calcite–chalcopyrite veins and biotite alteration, may suggest that a potassic fluid was responsible for leaching copper from epidote-altered metabasalts. This potassic fluid then deposited chalcopyrite in the overlying sedimentary rocks to form the Mount Isa copper deposit. Field observations suggest that potassic alteration on the regional scale is typically associated with K-feldspar veins and vesicle fill, whereas local mine-related, biotite-rich potassic alteration is confined to areas associated with a more reduced fluid consistent with the stability of ilmenite and pyrrhotite identified by Hannan et al. (1993). The reduced nature of the biotite- and chlorite-rich assemblages was attributed by Heinrich et al. (1995) to the advection of oxidised fluids from the metabasalts along the Paroo Fault and into the reduced Urquhart Shale, with minor back flow of the subsequently reduced fluid.

Proposed model

A two-stage model for the mobilisation and leaching of copper from the Eastern Creek Volcanics is proposed based on the regional geochemistry, iron–titanium oxide mineral chemistry and geochemical modelling presented in this study. Copper was released into metamorphic fluids at sites fluxed by CO_2, such as areas where metabasalts are juxtaposed or interleaved with carbonate-rich sedimentary rocks. Copper was released from actinolite–albite- and calcite–magnetite-dominated rocks, as shown by the depleted copper concentrations found in the Haslingden area compared with those in the less altered Gunpowder area. Metamorphic fluids carrying copper are interpreted to have migrated along permeable contacts such as sediment–basalt interfaces and flow tops, into zones of high fracture permeability, probably produced by the regional deformation (D_2) accompanying peak metamorphism.

Within these zones of high permeability, high fluid–rock ratios are interpreted to have resulted in extensive epidote metasomatism, resulting in epidote veining and replacement of the metabasalt groundmass mineralogy by epidote. Epidote vein relationships and orientations confirm epidote to be syn-metamorphic. Previous studies found contradictory timing relations for epidote veining, with both syn- and post-metamorphic textural relationships (Bain et al. 1992; Heinrich et al. 1995). This suggests that epidote alteration was a protracted event occurring throughout the regional metamorphic event. Chalcopyrite was deposited as intergrowths with epidote. This explains the gain in copper in epidote-altered rocks when compared with the Gunpowder area.

During the last phase of deformation which was coincident with copper deposition at Mount Isa, extensive reactivation and dilation of pre-existing structures, such as epidote veins, allowed oxidised hydrothermal fluids to interact with epidote-rich fracture zones. The existence of an oxidised hydrothermal fluid in the formation of the Mount Isa copper deposit has been suggested by several studies (e.g. Andrew et al. 1989; Heinrich et al. 1995; Wilde et al. 2005). Oxidised fluids are well documented for their ability to transport significant copper in solution (e.g. Haynes and Bloom 1987).

This fluid was likely to be oxidised and potassium rich, resulting in K-feldspar-bearing veins which overprint epidote-altered zones containing peak metamorphic chalcopyrite. The potassic fluid leached copper from the epidote-altered metabasalt sequence (as shown by the coincidence of potassium- and calcium-rich alteration zones in the regional geochemistry), retaining its oxidised state due to the oxidised nature of Fe-rich epidote-lined fractures, as also suggested by Heinrich et al. (1995), and therefore capable of carrying copper in solution. This process is supported by the occurrence of both copper-depleted and copper-enriched epidote-altered samples in the Haslingden area (Hannan et al. 1993; Heinrich et al. 1995). The oxidised, potassic and copper-rich fluid then flowed up the Paroo Fault and into the Urquhart Shale. Fluid flow along the Paroo Fault resulted in intense potassic metasomatism producing the biotite–ilmenite alteration that is observed beneath the copper deposit.

The metabasalts of the Hazeldene area differ from those in the Haslingden area in that they are dominated by the

Pickwick Metabasalt Member of the Eastern Creek Volcanics and have undergone upper greenschist to amphibolite facies metamorphism. Titanomagnetite in metabasalts from the Hazeldene area has broken down in varying degrees to form metamorphic magnetite and ilmenite. The copper content of the oxides has been preserved, if not increased, during this metamorphic process. The regional geochemistry is consistent with copper depletion from the Hazeldene area metabasalts, and this is associated with areas of high potassium (Table 6). Therefore, copper remobilisation did not occur during regional amphibolite facies metamorphism in the Hazeldene area possibly due to the absence of CO_2 which allowed the oxides and sulphides to remain stable. Post-metamorphic copper depletion of the metabasalt by potassium-rich fluids may have occurred.

Comparison with previous interpretations

The results of this study differ from previous work (Wyborn 1987; Bain et al. 1992; Hannan et al. 1993; Heinrich et al. 1995) in that in this contribution, regional greenschist facies metamorphism of the metabasalts is required before the leaching of copper from the sequence to pre-concentrate copper into highly permeable oxidised zones. Without this stage in the process, the oxidised ore-forming fluids would be: (1) reduced on interaction with the metabasalts, therefore reducing their capacity to transport copper, and (2) unable to interact with the majority of the metabasalt pile due to a lack of fracture permeability. Heinrich et al. (1995) noted the presence of syn-metamorphic epidote alteration as important for retaining the oxidation state of the fluid, but its exact role in the process was not defined.

The absence of syn-metamorphic pre-concentrations of copper does not preclude the possibility of ore deposit formation, but as seen from data for the Hazeldene area, the interaction of the ore-forming fluid and the metabasalt is limited without an oxidised fracture network, and there is an absence of economic copper deposits in this region.

The model proposed in this study provides some evidence towards the suggestion by Waring et al. (1998) that the Mount Isa copper deposit may be a high-temperature end member of sediment-hosted copper deposits. Under high-temperature conditions, fluids are only required to be moderately oxidised, such as those equilibrated with silicate rocks, to transport copper, whereas low-temperature diagenetic fluids are required to be highly oxidised to transport copper, hence the formation of red beds in typical sediment-hosted copper deposits (Waring et al. 1998). A model invoking leaching of metal from basaltic igneous rocks by oxidised fluids at Mount Isa has similarities with the giant sediment-hosted copper deposits worldwide. In the sediment-hosted Ngwako Pan copper deposit, Botswana, oxidised fluids circulated through red beds and became copper-rich where they passed through areas of basaltic rocks (Schwartz et al. 1995). Jowett (1986) found that major mineralisation in the Kupferschiefer correlated with basaltic rocks in the basement.

Mafic igneous metal source rocks are also implicated in other styles of copper mineralisation. Nd-isotope data from the Olympic Dam Fe-oxide Cu–Au deposit in South Australia provide evidence that oxidised ore fluids leached copper from both copper-rich mafic rocks and copper-poor granitic rocks (Johnson and McCulloch 1995). In the sediment-hosted Pb–Zn district of the McArthur Basin, northern Australia, K-metasomatism of mafic volcanic rocks by oxidised fluids resulted in significant leaching of base metals including copper (Cooke et al. 1998).

Copper mass balance

The evidence presented suggests that copper was leached from the Eastern Creek Volcanics and transported by fluids to form the Mount Isa copper orebodies. There is evidence for a 70% depletion in whole-rock copper from the K-altered Cromwell Metabasalt Member in the epidote-altered Haslingden area. Copper mass balance calculations can be used to calculate the volume of metabasalt required for leaching by potassic fluids to account for the 13 million tonnes of copper in the Mount Isa copper deposit (Perkins 1990). The following assumptions have been made for the purpose of calculations:

1. The amount of Cu leached is 119 ppm, assuming that the Cu content of the epidote-altered Cromwell Metabasalt was 171 ppm before potassic alteration and 52 ppm after potassic alteration (Table 6).
2. The specific gravity of the metabasalts is approximately 2.9 (Leaman 1991).

The mass balance calculation indicates that approximately 1.1×10^{11} tonnes of epidote-altered metabasalt is required to be leached of copper. This translates to a rock volume of 38 km^3 which spatially is an area of approximately 6.0×6.5 km assuming a 1-km-thick sequence of metabasalt. Potassic alteration associated with copper depletion (Fig. 9d) easily accounts for this area of altered metabasalt within the epidote-altered zones. Realistically, the efficiency of leaching would be significantly less than the calculation assumed; however, the area calculated is insignificant in comparison with the available epidote-altered metabasalts.

Conclusions

The Eastern Creek Volcanics are a potential source of copper for the giant sediment-hosted Mount Isa copper deposit. Laser ablation ICP-MS analyses of iron–titanium oxides within the metabasalts demonstrate that copper was mobilised during the metamorphic breakdown of magmatic titanomagnetite (and chalcopyrite) and growth of metamorphic magnetite. Copper hosted within titanomagnetite is not incorporated into metamorphic magnetite, and petrology and geochemical modelling suggest that this

copper could have precipitated with syn-metamorphic epidote.

The epidote alteration zones refractured due to post-metamorphic deformation, which allowed oxidised potassium-rich fluids to remobilise copper from the Eastern Creek Volcanics and ultimately deposit some of it in the overlying reduced sedimentary rocks. The oxidised nature of epidote allowed the fluid to remain oxidised and therefore carry significant concentrations of copper in solution. Potassium-rich phases such as K-feldspar represent the regional expression of the ore-forming fluid.

The derivation of copper from mafic rocks, deduced in this model, has also been interpreted for some other world-class sediment-hosted copper deposits. Determining the spectrum of conditions which produce copper mobility from mafic source rocks will in the future produce greater understanding of relationships between the major sediment-hosted copper deposit styles.

Acknowledgements The work reported in this study was conducted as part of the predictive mineral discovery Cooperative Research Centre, with support from Xstrata Copper, and this paper is published with the permission of the CEO. I wish to thank Andy Wilde, Lucy Chapman, David Cooke, Robert Duncan, Frank Bierlein, Geordie Mark, Mike Rubenach and two anonymous Mineralium Deposita reviewers for their many suggestions that led to significant improvements to this paper.

References

Andrew AS, Heinrich CA, Wilkins RWT, Patterson DJ (1989) Sulfur isotope systematics of copper ore formation at Mount Isa, Australia. Econ Geol 84:1614–1626

Bain JHC, Heinrich CA, Henderson GAM (1992) Stratigraphy, structure, and metasomatism of the Haslingden Group, east Moondarra area, Mount Isa: a deformed and mineralised Proterozoic multistage rift-sag sequence. In: Stewart AJ, Blake DH (eds) Detailed studies of the Mount Isa Inlier; Australian Geological Survey Organisation Bulletin 243, pp 125–136

Bethke CM (1998) The Geochemist's Workbench. University of Illinois, IL

Blake DH, Stewart AJ (1992) Stratigraphic and tectonic framework, Mount Isa Inlier. In: Stewart AJ, Blake DH (eds) Detailed studies of the Mount Isa Inlier; Australian Geological Survey Organisation Bulletin 243. Australian Government Publishing Service, Canberra, pp 1–11

Bultitude RJ, Wyborn LAI (1982) Distribution and geochemistry of volcanic rocks in the Duchess-Urandangi region, Queensland. BMR J Aust Geol Geophys 7:99–112

Cassidy KF, Groves DI, Binns RA (1988) Manganoan ilmenite formed during regional metamorphism of Archean mafic and ultramafic rocks from Western Australia. Can Mineral 26:999–1012

Connors KA, Page RW (1995) Relationships between magmatism, metamorphism and deformation in the western Mount Isa Inlier, Australia. Precambrian Res 71:131–153

Connors KA, Proffett JM, Lister G, Scott RJ, Oliver NHS, Young D (1992) Geology of the Mount Novit Ranges, southwest of Mount Isa mine. In: Stewart AJ, Blake DH (eds) Detailed studies of the Mount Isa Inlier; Australian Geological Survey Organisation Bulletin 243, pp 137–160

Cooke DR, Bull SW, Donovan S, Rogers JR (1998) K-metasomatism and base metal depletion in volcanic rocks from the McArthur Basin, Northern Territory—implications for base metal mineralization. Econ Geol 93:1237–1263

Crocket JH (2002) Platinum-group element geochemistry of mafic and ultramafic rocks. In: Cabri LJ (ed) The geology, geochemistry, mineralogy and mineral beneficiation of platinum-group elements. Canadian Institute of Mining, Metallurgy and Petroleum, Canada, pp 177–210

Derrick GM (1976) Mary Kathleen, Queensland 1:100,000 geological map. Geoscience Australia, Canberra

Duncan RJ, Wilde AR, Bassano K, Maas R (2006) Geochronological constraints on tourmaline formation in the Western Fold Belt of the Mount Isa Inlier, Australia: evidence for large-scale metamorphism at 1.57 Ga? Precambrian Res 146:120–137

Farquharson RB, Richards JR (1974) U–Th–Pb isotope systematics related to igneous rocks and ore Pb, Mount Isa, Queensland. Miner Depos 9:339–356

Frietsch R (1970) Trace elements in magnetite and hematite mainly from northern Sweden, Aarsbok. Sveriges Geologiska Undersoekning 64:136

Frost BR, Lindsley DH (1991) Occurrence of iron–titanium oxides in igneous rocks. In: Lindsley DH (ed) Oxide minerals: petrologic and magnetic significance. Rev Miner 25:433–468

Goldschmidt VM (1954) Geochemistry. Oxford University Press, London

Grant JA (1986) The isocon diagram—a simple solution to Gresens' equation for metasomatic alteration. Econ Geol 81:1976–1982

Gregory MJ (2005) The geological evolution of the Eastern Creek Volcanics, Mount Isa, Australia and implications for the Mount Isa copper deposit. Ph.D. thesis, Monash University, Melbourne

Gulson BL, Perkins WG, Mizon KJ (1983) Lead isotope studies bearing on the genesis of copper orebodies at Mount Isa, Queensland. Econ Geol 78:1466–1504

Hand M, Rubatto D (2002) The scale of the thermal problem in the Mt. Isa Inlier. In: Preiss VP (ed) Geoscience 2002: expanding horizons. 16th Australian geological convention, Adelaide, South Australia, pp 173

Hannan KW, Golding SD, Herbert HK, Krouse HR (1993) Contrasting alteration assemblages in metabasites from Mount Isa, Queensland; implications for copper ore genesis. Econ Geol 88:1135–1175

Haynes DW, Bloom MS (1987) Stratiform copper deposits hosted by low-energy sediments: III. Aspects of metal transport. Econ Geol 82:635–648

Heinrich CA, Bain JHC, Mernagh TP, Wyborn LAI, Andrew AS, Waring CL (1995) Fluid and mass transfer during metabasalt alteration and copper mineralization at Mount Isa, Australia. Econ Geol 90:705–730

Hill RM (1978) Mount Isa Queensland 1:100,000 geological map. Geoscience Australia, Canberra

Johnson JP, McCulloch MT (1995) Sources of mineralising fluids for the Olympic Dam deposit (South Australia): Sm–Nd isotopic constraints. Chem Geol 121:177–199

Jowett EC (1986) Genesis of Kupferschiefer Cu–Ag deposits by convective flow of Rotliegende brines during Triassic rifting. Econ Geol 81:1823–1837

Leaman DE (1991) Geophysical constraints on structure and alteration of the Eastern Creek Volcanics, Mt. Isa, Queensland. Aust J Earth Sci 38:457–472

Lister GS, O'Dea MG, Somaia I (1999) A tale of two synclines; rifting, inversion and transpressional popouts at Lake Julius, northwestern Mt. Isa Terrane, Queensland. Aust J Earth Sci 46:233–250

Muir MD (1981) The microfossils from the Proterozoic Urquhart Shale, Mount Isa, Queensland, and their significance in relation to the depositional environment, diagenesis, and mineralisation. Minera Depos 16:51–58

Neudert MK, Russell RE (1981) Shallow water and hypersaline features from the middle Proterozoic Mt. Isa sequence. Nature 293:284–286

Neumann N, Southgate PN, McIntyre A, Gibson G (2005) New data on rock ages from Mt. Isa Inlier. AUSGEO News 78

O'Dea MG, Lister G, MacCready T, Betts PG, Oliver NHS, Pound KS, Huang W, Valenta RK (1997) Geodynamic evolution of the Proterozoic Mount Isa terrain. In: Burg J-P, Ford M (eds) Orogeny through time. Geol Soc Lond Spec Publ 121:99–122

Page RW, Sweet IP (1998) Geochronology of basin phases in the western Mt. Isa Inlier, and correlation with the McArthur Basin —application of radiogenic isotopes to the study of Australian ore deposits. Aust J Earth Sci 45:219–232

Page RW, Jackson MJ, Krassay AA (2000) Constraining sequence stratigraphy in North Australian basins; SHRIMP U–Pb zircon geochronology between Mt. Isa and McArthur River. Aust J Earth Sci 47:431–459

Painter MGM, Golding SD, Hannan KW, Neudert MK (1999) Sedimentologic, petrographic, and sulfur isotope constraints on fine-grained pyrite formation at Mount Isa Mine and environs, Northwest Queensland, Australia. Econ Geol 94:883–912

Pearce NJG, Perkins WT, Westgate JA, Gorton MP, Jackson SE, Neal CR, Chenery SP (1997) A compilation of new and published major and trace element data for NIST SRM 610 and NIST SRM 612 glass reference materials. Geostand Newsl 21:115–144

Perkins WG (1984) Mount Isa silica dolomite and copper orebodies; the result of a syntectonic hydrothermal alteration system. Econ Geol 79:601–637

Perkins WG (1990) Mount Isa copper orebodies. In: Hughes FE (ed) Geology of the mineral deposits of Australia and Papua New Guinea. Australasian Institute of Mining and Metallurgy, pp 935–941

Perkins C, Heinrich CA, Wyborn LAI (1999) $^{40}Ar/^{39}Ar$ geochronology of copper mineralization and regional alteration, Mount Isa, Australia. Econ Geol 94:23–36

Phillips GN, Evans KA (2004) Role of CO2 in the formation of gold deposits. Nature 429:860–863

Rubenach MJ (1992) Proterozoic low-pressure/high-temperature metamorphism and an anticlockwise P–T–t path for the Hazeldene area, Mount Isa Inlier, Queensland, Australia. J Metamorph Geol 10:333–346

Schwartz MO, Akanyang P, Trippler K, Ngwisanyi TH (1995) The sediment-hosted Ngwako Pan Copper Deposit, Botswana. Econ Geol 90:1118–1147

Shvarov Y, Bastrakov E (1999) HCh: a software package of geochemical equilibrium modelling. User's guide. Australian Geological Survey Organisation, Canberra

Smith SE, Walker KR (1971) Primary element dispersions associated with mineralization at Mount Isa, Queensland. Bulletin-Australia, Bureau of Mineral Resources, Geology and Geophysics 131

Swager CP (1985) Syndeformational carbonate-replacement model for the copper mineralization at Mount Isa, Northwest Queensland; a microstructural study. Econ Geol 80:107–125

Valenta R (1994) Syntectonic discordant copper mineralization in the Hilton Mine, Mount Isa. Econ Geol 89:1031–1052

van Achterbergh E, Ryan CG, Jackson SE, Griffin WL (2001) Data reduction software for LA-ICP-MS. In: Sylvester P (ed) Laser ablation-ICPMS in the Earth Sciences. Mineral Association of Canada Short Course Handbook 29, pp 239–243

Waring CL (1990) The genesis of the Mount Isa copper orebodies. Ph.D. thesis, Monash University, Melbourne

Waring CL, Heinrich CA, Wall VJ (1998) Proterozoic metamorphic copper deposits. AGSO J Aust Geol Geophys 17:239–246

Wilde AR, Gregory MJ, Duncan RJ, Gessner K, Kuhn M, Jones PA (2005) Geochemical process model for the Mt. Isa Cu–Co–Ag deposits. In: Mao J, Bierlein F (eds) Eight biennial SGA meeting–mineral deposit research: meeting the global challenge, Beijing, China, pp 199–202

Wilson IH, Derrick GM, Perkin DJ (1985) Eastern Creek Volcanics; their geochemistry and possible role in copper mineralisation at Mount Isa, Queensland. BMR J Aust Geol Geophys 9:317–328

Wyborn LAI (1987) The petrology and geochemistry of alteration assemblages in the Eastern Creek Volcanics, as a guide to copper and uranium mobility associated with regional metamorphism and deformation, Mount Isa, Queensland. In: Pharaoh TC, Beckinsale RD, Rickard DT (eds) Geochemistry and mineralization of Proterozoic Volcanic Suites, Keyworth, United Kingdom, pp 425–434